

This is the Post-print version of the following article: *Litza Halla Velazquez-Jimenez, Esmeralda Vences-Alvarez, Jose Luis Flores-Arciniega, Horacio Flores-Zuñiga, Jose Rene Rangel-Mendez, Water defluoridation with special emphasis on adsorbents-containing metal oxides and/or hydroxides: A review, Separation and Purification Technology, Volume 150, 2015, Pages 292-307*, which has been published in final form at: <https://doi.org/10.1016/j.seppur.2015.07.006>

© 2015. This manuscript version is made available under the Creative Commons Attribution-NonCommercial-NoDerivatives 4.0 International (CC BY-NC-ND 4.0) license <http://creativecommons.org/licenses/by-nc-nd/4.0/>

Accepted Manuscript

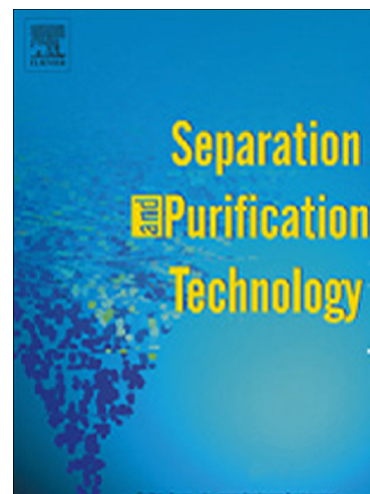
Water defluoridation with special emphasis on adsorbents-containing metal oxides and/or hydroxides: a review

Velazquez-Jimenez Litza Halla, Vences-Alvarez Esmeralda, Flores-Arciniega Jose Luis, Flores-Zuñiga Horacio, Rangel-Mendez Jose Rene

PII: S1383-5866(15)30077-0
DOI: <http://dx.doi.org/10.1016/j.seppur.2015.07.006>
Reference: SEPPUR 12422

To appear in: *Separation and Purification Technology*

Received Date: 6 March 2015
Revised Date: 26 June 2015
Accepted Date: 5 July 2015



Please cite this article as: V.L. Halla, V-A. Esmeralda, F.J. Luis, F-Z. Horacio, R.J. Rene, Water defluoridation with special emphasis on adsorbents-containing metal oxides and/or hydroxides: a review, *Separation and Purification Technology* (2015), doi: <http://dx.doi.org/10.1016/j.seppur.2015.07.006>

This is a PDF file of an unedited manuscript that has been accepted for publication. As a service to our customers we are providing this early version of the manuscript. The manuscript will undergo copyediting, typesetting, and review of the resulting proof before it is published in its final form. Please note that during the production process errors may be discovered which could affect the content, and all legal disclaimers that apply to the journal pertain.

Water defluoridation with special emphasis on adsorbents-containing metal oxides and/or hydroxides: a review

Velazquez-Jimenez Litza Halla^a, Vences-Alvarez Esmeralda^a, Flores-Arciniega Jose Luis^b, Flores-Zuñiga Horacio^b, Rangel-Mendez Jose Rene^{a*}

^aDivision of Environmental Sciences and ^bDivision of Advanced Materials; Instituto Potosino de Investigación Científica y Tecnológica, A.C., Camino a la Presa San José 2055, Col. Lomas 4a sección, C.P. 78216, San Luis Potosí, S.L.P., México.

Abstract

Fluoride contamination in drinking water has been recognized as one of the major worldwide problems since this represents a serious threat to human health. The World Health Organization (WHO) recommends the guideline value (maximum permissible limit) of 1.5 mg L^{-1} for fluoride in drinking water. Unfortunately, many countries have high fluoride concentrations (up to 30 mg L^{-1}) in water supplies that may cause widespread fluorosis and skeletal illnesses among the population. Many methods have been developed for fluoride removal from water including adsorption, ion exchange, electrodialysis and precipitation. Nevertheless, more efficient and cost-effective processes and materials are needed to comply with the fluoride maximum permissible limit. Adsorption has been widely used because it is the most cost-effective methodology for the removal of ionic contaminants from aqueous solutions. Various adsorbent materials have been used to remove fluoride from water, for instance activated alumina, activated carbon, bone char, minerals, among others, but unfortunately their chemical stability and/or selectivity and adsorption capacity is something that still has to improve substantially. During the last decade, metal oxyhydroxides in powder form and supported on different matrixes have been of great interest for fluoride removal. This review condenses the advances on this last topic that is still under study.

Key words: fluoride, adsorption, metal oxyhydroxides, water treatment.

1. Introduction

Fluoride source occurs in a geological environment. Minerals like sellaite (MgF_2), fluorspar (CaF_2), cryolite (Na_3AlF_6) and fluorapatite [$3\text{Ca}_3(\text{PO}_4)_2\text{Ca}(\text{F},\text{Cl}_2)$] can release fluoride ions (F^-) when the conditions of temperature, pH, anion-exchange, among others, favor their dissolution [1]. The occurrence of F^- in groundwater is also due to the anthropogenic discharges from commercial and/or domestic activities, and from industry (i.e. semiconductor manufacturing, glass and ceramic production, uranium and aluminum refinement, toothpaste, fertilizer, electroplating, etc.).

37 At present, groundwater is the primary source of drinking water for roughly 30 percent of the world's
38 population and is often the main source of fluoride intake by humans in areas where fluorosis is endemic
39 [2]. The relationship of fluoride-human health is quite extensive, and is focused on the adverse effects on
40 teeth and bones (dental and skeletal fluorosis), DNA structure (genetic mutations, birth defects), and
41 illnesses spread (cancer, Alzheimer disease, renal and neurological damage), among others [3].

42 Fluoride is considered beneficial at levels around of 0.7 mg L^{-1} but it is hazardous if it exceeds 1.5
43 mg L^{-1} , which is the World Health Organization (WHO) limit in drinking water and this is followed in
44 most nations. High fluoride concentrations in groundwater, up to 30 mg L^{-1} , can be found in many parts of
45 the world, and is endemic in at least 25 countries across the globe [4-6]. The most affected areas are parts
46 of China, India, Sri Lanka, South Africa, and in less proportion in rural and semi-urban areas of United
47 States of America, central Europe, northern Mexico and central Argentina. This problem is exacerbated by
48 the need to drink more water because of the heat and dry climates, and the limited water resources in
49 Third World countries. Even in developed nations, fluoride removal (or defluoridation) from public
50 drinking water supplies has been a contentious issue that ends in more stringent fluoride limits [7]. Efforts
51 to reduce fluoride from drinking water to acceptable limits are essential, which require a great deal of
52 investment in research. There are several methods and techniques that can be employed for water
53 defluoridation (precipitation/coagulation, ion-exchange, membrane technique, etc.), and its choice
54 depends on the fluoride ions concentration, existing treatment processes, treatment costs, handling of
55 residuals and versatility of the given technique [8]. However, these methods have some limitations like
56 performance, production of waste, and high costs of installation. Adsorption has shown to be a better
57 choice to remove pollutants from water, such as fluoride ions, because of its lower cost, flexibility and
58 simplicity of design, high efficiency, and high selectivity [9]. A variety of adsorbent materials have been
59 used to remove fluoride from water, such as carbon based adsorbents, agricultural and industrial wastes,
60 metallic oxides and hydroxides or oxyhydroxides [8-13]. Nevertheless, recent developments have
61 discovered that metals, in their form of oxides or oxyhydroxides, by their selves or loaded in several
62 materials are good candidates to remove fluoride from water. Unfortunately, this knowledge is dispersed
63 in the literature, hence, the aim of this review is to condense the most relevant studies on fluoride removal
64 from water by adsorption, emphasizing the novel metal oxide/oxyhydroxides adsorbent materials.

65

66 **2. Technologies for fluoride removal from water**

67 Several techniques have been developed in order to decrease the fluoride concentration to safe limits
68 in water supplies. Defluoridation methods, based on the nature of the type of process involved, can be
69 generally grouped into precipitation/coagulation, adsorption and/or ion exchange, and filtration by
70 membranes. The principle involved in precipitation-coagulation technology is that the fluoride ions adsorb

71 on the flocs and are then subsequently removed either simultaneous or in succeeding treatment units such
72 as sedimentation, fixed beds or microfiltration units. On the other hand, adsorption is characterized by the
73 use of adsorbents where fluoride is concentrated and removed from water. Parameters such as pH,
74 temperature, and interfering anions have been considered in this research topic since they can greatly
75 affect the adsorption process [10]. The adsorbent materials include activated carbon, activated alumina,
76 ion-exchange resins, fly ash, clay, minerals, soils, among others [11]. On the other hand, membrane
77 techniques involve the use of semi-permeable membranes that are briefly discussed in section 2.2.

78 2.1 Precipitation/coagulation

79 Coagulation with aluminum salts has been employed for a long time to remove fluoride ions [12,
80 13]. Coprecipitation or adsorption may occur when Al(III) ions are added to fluoride-containing water.
81 The efficiency of the removal of fluoride by a fixed amount of aluminum salt depends on pH, alkalinity,
82 the coexisting anions, and other solution characteristics [14]. The most appropriate pH for defluoridation
83 using the coagulation technique is 5.5–6.5 [15]. Nalgonda technique, is one of the most popular
84 defluoridation methods in countries like India, Kenya, Tanzania and Senegal, it involves the addition of
85 calculated quantities of alum, lime and bleaching powder to the water. After the mixing, the water is
86 processed with flocculation, sedimentation, filtration and disinfection [11]. Nevertheless, this technique
87 presents several disadvantages like a high concentration of SO_4^{2-} ions and residual aluminum levels in the
88 treated water.

89 On the other hand, the electrocoagulation (EC) process utilizes “sacrificed” anodes to form an
90 active coagulant which is used to remove the pollutant by precipitation and flotation *in situ*. Compared
91 with traditional chemical coagulation (CC), the electrocoagulation process requires less space and does
92 not require chemical storage, dilution, and pH adjustment [16]. It is proven to be effective in water
93 treatment system for small or medium size communities [17].

94 Although many studies have investigated the removal of fluoride by aluminum (Al) coagulation,
95 few studies have been focused on the effects of colloids, such as kaolin suspensions. Lui et al., [18]
96 studied the effects of fluoride at different molar ratios of fluoride to Al ($R_{\text{F:Al}}$) on turbidity removal, zeta
97 potential, flocs growth, and residual Al levels in a series of batch experiments. The authors found that at
98 insufficient Al doses, the fluoride showed adverse effects at $R_{\text{F:Al}}$ above 10:10, whereas the opposite effect
99 was observed at $R_{\text{F:Al}}$ below 2:10 at $\text{pH} < 8$. At pH greater than 8, little effect was observed over a wide
100 $R_{\text{F:Al}}$ range of 1:10 to 30:30. The adverse effects of fluoride were related to the decrease of zeta potential,
101 smaller flocs and elevated levels of Al residual. Moreover, this study indicated that after adsorbing
102 fluoride, the freshly-prepared aluminum hydroxides (*in-situ* $\text{Al}_2\text{O}_3 \cdot \text{H}_2\text{O}$) that were spent may be reclaimed
103 as coagulant for colloid removal after being dissolved by an acid solution. Some other researchers such as
104 Hu et al., [19] studied the effect of the molar ratio of hydroxide and fluoride ions ($\gamma\text{-OH}$ and γF) with

105 respect to Al(III) ions in coagulation and electrocoagulation (EC). This study showed that the efficiency of
106 defluoridation was approximately 100% when the sum of γ -OH and γ F (γ -OH+F) was close to 3. This
107 finding reveals that fluoride and $-\text{OH}$ ions can co-precipitate with Al(III) ions and develop $\text{Al}_n\text{F}_m(\text{OH})_{3n-m}$.

108 Also, Sujana et al., [20] studied the removal of fluoride from aqueous solution by using aluminum
109 sludge. This study considered the contact time, the adsorbent and adsorbate concentration, temperature,
110 pH, and the effect of the concentrations of other anions. The treated alum showed a heterogeneous surface
111 in nature which was reflected in the heterogeneous binding sites. The optimum pH for complete removal
112 of fluoride ions was 6, the adsorption rate was faster during the initial 5 minutes and the equilibrium was
113 reached within 240 minutes. The adsorption process followed a first-order kinetics and could be affected
114 with an increase in temperature from 307 to 337 K, besides, defluoridation in the presence of phosphate
115 and silicate at $10\text{-}50\text{ mg L}^{-1}$ has an adverse effect on the fluoride removal. Furthermore, Zhu et al., [21]
116 used a new approach to investigate fluoride distribution in the defluoridation process by
117 electrocoagulation, which was divided into three parts: remained in water, removal by electrodes, and
118 adsorption on hydroxide aluminum flocs. The fluoride distribution was investigated in terms of various
119 critical parameters such as pH, charge loading, current density and the initial concentration of fluoride.
120 The results demonstrated that defluoridation can be performed with high efficiency between pH 6.0-7.0,
121 and would become dominant even under basic conditions ($\text{pH} \geq 7.5$). The optimal charge loading and
122 current density were established at $4.15\text{ Faradays m}^{-3}$ and $9.26\text{ Amperes m}^{-2}$, respectively. The general
123 relation between the overall defluoridation efficiency and initial F^- concentration decreased from 92 to
124 80% while the range increased from 3 to 15 mg L^{-1} . A chemical complex of $\text{Al}_n(\text{OH})_m\text{F}_k^{3n-m-k}$ was
125 formulated to explain the mechanism inside the EC defluoridation process. Following with the
126 electrocoagulation process, Hu et al., [22] developed a variable order kinetic (VOK) model derived from
127 the Langmuir equation to simulate the fluoride removal kinetics by electrocoagulation with bipolar
128 aluminum electrodes. The results showed that parameters Γ_{max} and k for the VOK model were constant
129 when the initial fluoride concentration varied. On the other hand, they observed that the current efficiency
130 is independent upon initial fluoride concentration but this varies with current density. Therefore, their
131 results revealed good agreement between the predictive equation and the experimental data. However,
132 they found limitations in the VOK model since this could not simulate systems with an initial acidity of
133 0.5 or 1.0 mM and with a high initial fluoride concentration.

134 Moreover, Gong et al., [23] studied the effects of aluminum fluoride complexes by a series of batch
135 experiments. The transformation of the fluoride species in coagulation was studied by a simultaneous
136 determination of free fluoride and total fluoride at different pH and fluoride concentrations. For total
137 fluoride removal, the optimal pH was 7.0, and up to this value complexes were completely dissociated to
138 free fluoride. Comparison between coagulation with complexation and adsorption by $\text{Al}(\text{OH})_3$ flocs

139 demonstrated that coagulation shows higher fluoride removal efficiency between pH 6.0 and 9.0, and the
140 process of coagulation involved an Al-F complexation, an Al hydrolysis and a precipitation. During the
141 adsorption process, the fluoride was removed by an ion exchange with $-OH$. Besides, it was implied that
142 I-F complexation promotes fluoride removal in coagulation. Furthermore, the characterization by FTIR
143 and XPS also showed that Al-F-OH co-precipitates in coagulation.

144

145 **2.2 Membrane Processes**

146 Membrane processes imply the use of a semi-permeable membrane as an interphase between adjacent
147 phases, and acts as a barrier controlling material transport between them. The driving force to transport in
148 membrane separation is generally a difference in chemical potential created due to a concentration or
149 pressure gradient across the membrane, or by an electric field. Two important phenomena that
150 significantly reduce membrane permeability and selectivity are concentration polarization and membrane
151 fouling. Membrane techniques like reverse osmosis, nanofiltration, dialysis and electrodialysis have been
152 applied industrially in fields ranging from medicine to the chemical industries in the removal of inorganic
153 ions, being one of them fluoride [24]. The use of these techniques can be very attractive for water
154 treatment processes to avoid some difficulties that precipitation, coagulation and adsorption may present
155 during their use.

156

157 **2.2.1 Reverse osmosis**

158 Reverse osmosis produces extremely pure water. This is a physical process in which contaminants are
159 removed by applying higher pressure on the feedwater to direct it through a semipermeable membrane
160 (see Figure 1). The process is the reverse of natural osmosis as a result of the applied pressure to the
161 concentrated side. The current applications are in desalination of drinking water and water purification for
162 microelectronics and medical uses, because it rejects all dissolved solids. The factors that usually
163 influence the membrane selection are the cost, recovery, rejection, water characteristics to treat,
164 temperature, and pressure, among others. Defluoridation using reverse osmosis systems is running
165 successfully in many developed countries [24].

166 Arora et al., [25] evaluated the potential of a reverse osmosis membrane for fluoride removal of
167 underground water samples from India, at concentrations between 2.5 to 10 mg L⁻¹. The results indicated
168 that reverse osmosis membranes removed up to 95% of F⁻, and there was no need to remineralize the
169 water. Besides, at pH >7 the efficiency decreased, but in acidic pH the performance of the membrane was
170 affected and needed to be replaced, on the other hand, Ndiaye et al., [26] studied fluoride removal from
171 effluents of the electronic industry using reverse osmosis. The results showed that the rejection of fluoride
172 was typically higher than 98%, considering that the membranes used in the study were fully regenerated

173 after each set of experiments. For industrial effluents, the process developed in this research allowed the
174 reduction of the treated volume from 6 to 0.36 m³ d⁻¹ without any pretreatment. Taking into account that
175 membranes are sensitive to the polarization phenomena, and that they tend to forward biological fouling
176 due to natural organic matter and microorganisms; mineral fouling can also occur when salts exceed and
177 tend to precipitate [24]. In this respect Nicolas et al., [27] optimized the softening pretreatment, by sodium
178 carbonate, of brackish water contaminated with high concentration of fluoride (> 5 mg L⁻¹) in order to
179 obtain purified water by reverse osmosis in a second stage: the calculated optimal amount of softening
180 chemical was 15 mmol L⁻¹ of Na. Additionally, the pretreatment allowed not only an almost total removal
181 of calcium but also a partial elimination of magnesium and fluoride.

182 2.2.2 Dialysis and Electrodialysis

183 Dialysis and electrodialysis are similar to reverse osmosis. In the case of dialysis, one or more solutes
184 are transferred from one solution, called the feed, to another solution called the dialysate, through a
185 membrane due to a concentration gradient. In electrodialysis, the separation of components of an ionic
186 solution occurs in a cell consisting of a series of anion and cation-exchange membranes. These are
187 arranged in an alternate manner between an anode and a cathode to form individual electro-dialysis cells.
188 During the process of electrodialysis, there is an increase in the ion concentration of one type in one type
189 of component and it is accompanied by a simultaneous decrease in the concentration of the other type of
190 component (see Figure 2) [28].

191 Hichour et al., [29] used contaminated water samples from Africa (Maghreb, Senegal), to study the
192 removal of fluoride with the Donnan dialysis process in a counter flow system. To maintain the fluoride
193 concentration below the acceptable values (1.5 mg L⁻¹) at the outlet of the feed compartment, the extracted
194 fluoride ions were complexed by adding Al³⁺ into the receiver solution. Lounici et al., [30] also studied the
195 fluoride removal by using electrodialysis. Their results showed that desorption of fluoride from activated
196 alumina is a rapid process, within 6-15 min. Also, a study of adsorption-regeneration cycles showed that
197 the electrochemical technique was more efficient than commercial caustic soda with 95% of fluoride
198 removal. Following the same Donnan analysis, Germes et al., [31] also applied a hybrid process that
199 combines adsorption on aluminum (Al₂O₃) and zirconium oxide (ZrO₂) to treat groundwater with 4 mg L⁻¹
200 of fluoride concentration resulting from phosphate mining in Morocco. It was found that the fluoride
201 equilibrium concentration was attained more quickly and higher with ZrO₂ than with Al₂O₃. The
202 mineralization of the treated groundwater was not modified. The cation composition remained unchanged,
203 whereas anions (except chloride) were partially eliminated and substituted by Cl⁻. The above lead to a
204 fluoride concentration below 1.5 mg L⁻¹.

205 An interesting study by Annouar et al., [32] reported the elimination of fluorides from underground
206 water by adsorption on chitosan followed by electrodialysis with the help of CMX-ACS membranes. Both

207 methodologies approached a safe limit of fluoride concentration. Following the same route, Sahli et al.,
208 [33] studied the defluoridation of brackish groundwater in Morocco by electrodialysis. This research
209 group demonstrated that this methodology can defluorinate water with 3000 mg L⁻¹ of total dissolved salts
210 and 3 mg L⁻¹ of fluoride. Recently, Elazhar et al., [34] compared the performance of nanofiltration and
211 electrodialysis in fluoride removal from Moroccan groundwater. Although the performances are
212 comparable in both technologies, the study revealed that electrodialysis has the advantage of flexibility
213 with respect to the seasonal variation of fluoride content, and the final salt concentration can be adjusted.
214 Nevertheless, nanofiltration can be used for small-scale applications.

215

216 2.2.3 Nanofiltration

217 Nanofiltration is not often used in water treatment, but can compete with reverse osmosis and
218 electrodialysis for defluoridation of water supplies. The membranes that use this technology have
219 narrower pores than those used for reverse osmosis, and offer less resistance when the solutes pass
220 through them. As a consequence, the pressure required is much lower, less energy requirements, removal
221 of the solute is much less exhaustive, and flows are faster. Nanofiltration is generally used to remove
222 divalent ions such SO₄²⁻ and Ca²⁺, but it also can remove F⁻ from aqueous solutions despite being a very
223 small anion. Moreover, fluoride removal with this technique is possible due to its high charge density that
224 makes it a more strongly hydrated ion than others, and thus, it is more strongly retained in nanofiltration
225 membranes by steric effects. The selectivity of nanofiltration in comparison with reverse osmosis is also
226 an advantage due to the low cost of membrane materials that contributes to its actual spread. Furthermore,
227 nanofiltration (as well as electrodialysis) is more suitable for producing drinking water directly without
228 the need of remineralization. The main difference between nanofiltration and electrodialysis is that the
229 second one requires regeneration of ion-exchange membranes thus making its use more expensive than
230 nanofiltration.

231 As reported by Mohapatra et al., [35], several studies have been carried out using nanofiltration for
232 demineralization of water, especially in the defluoridation of brackish water and wastewater treatment
233 processes. Elazhar et al., [36] evaluated the use of nanofiltration to remove fluoride of 2400 m³ d⁻¹ of
234 water from a rural location in Morocco. The recovery rate obtained with this methodology was 84% of
235 water and a fluoride rejection of 97.8%. Recently, Nasr et al., [37] applied nanofiltration for defluoridation
236 of groundwaters. This study used commercial nanofiltration membranes and evaluated, among fluoride
237 removal, the influence of chloride, sulfate and calcium that usually co-exist in groundwater. The results
238 indicated that it is important to select an appropriate membrane in order to maintain Cl⁻ concentration in
239 acceptable levels without losing the selective ability to remove F⁻, mixing with groundwater or
240 remineralization is obligatory to produce water with a satisfactory composition.

241

242 **2.3 Ion exchange technologies**

243 Looking back in time it can be seen how synthetic resins, anionic and cationic, are compared in
244 fluoride removal. An example is given by Ku et al., [38], who found that anionic resins are more easily
245 interfered by the presence of foreign ions and are more difficult to be regenerated than cationic resins. The
246 experiments were performed with Amberlite IR-120 which fluoride removal efficiency was highly
247 affected by a pH increase. Essentially, the ion exchange technologies remain unchanged in terms of
248 advantages and disadvantages; although they have high removal efficiency their cost is always high. Also
249 the efficiency in fluoride removal decreases in the presence of other anions, in some cases pH changes and
250 the process is very dependent on the concentration of the ion of interest, in this case, F⁻ ion (Singh et al.)
251 [39].

252 In many cases the type of material for the membrane or resin is organic with a certain nature (cationic
253 or anionic) and it can function as a matrix for other ions. There are a lot of studies where materials are
254 employed as enhancers for defluoridation capacity over a certain type of membrane or resin. Classical
255 materials in water treatment as zeolite or activated carbon have been employed as ion exchangers.
256 Furthermore, in the case of zeolite due to its large internal surface area and active sites for fluoride
257 adsorption by exchanging Na⁺ bound zeolite with Al³⁺ or La³⁺ ions, as reported by Onyango et al. [40].

258 A new strategy seems to be the inclusion of metals in certain matrixes to increase the efficiency and
259 selectivity toward fluoride ions. One example is reported by Pan et al., [41], who synthesized a
260 polystyrene anion exchanger that supported hydrous zirconium oxide nanoparticles. Another example is a
261 chemically modified resin with Na⁺ and Al³⁺ (Viswanathan and S. Meenakshi [42]), that increased two
262 times the fluoride uptake.

263

264 **2.4 Adsorption process**

265 As previously mentioned, ion exchange, electrodialysis and membrane processes are effective and
266 can remove fluoride to a suitable level, however, they are considered a high cost water treatment method
267 and require frequent regeneration and cleaning of the scaling fouling [43,44]. Some advantages and
268 shortcomings of the water treatment techniques usually implemented to remove fluoride from water are
269 reported in Table 1. Adsorption is widely used, especially in developing countries. Industrialized countries
270 generally use more efficient but more costly adsorption media including synthetic ion resins or composite
271 materials combined with reverse osmosis and electrodialysis, while developing countries exploit
272 inexpensive locally available adsorptive media like clays, muds or agro-waste materials [13, 45]. As can
273 be seen, adsorption greatly dependent on the development of adsorptive materials, where the efficiency
274 of this technique mainly depends on adsorbents.

275 Recent attention of scientists has been devoted to the study of low cost, but effective conventional
276 and non-conventional materials. A large number of adsorbent materials have been tested, such as
277 amorphous alumina [46], activated alumina [47], activated carbon [48], calcite [49], clay [50], and rare
278 earth oxides [51, 52]. Besides, some adsorbents can only work at a certain acid pH value, such as activated
279 carbon which is only effective for fluoride removal at pH less than 3 [53].

280 Many researchers have developed synthetic sorbents using single or multi-metal oxides/hydroxides
281 for fluoride removal from water, as it will be discussed in the following sections. This review has been
282 focused on the potential of metal oxides/hydroxides/oxyhydroxides, and mixed metal oxides for water
283 defluoridation. The following sections, will present a summary of relevant research in this field in terms of
284 adsorption capacities and kinetics.

285

286 **2.4.1 Metallic based adsorbents**

287 These kinds of adsorbents have attracted more attention in recent years due to their high efficiency
288 in almost all of the cases that these were tested for fluoride removal. One of the main obstacles for their
289 implementation is their cost, however, it has been proven that small amounts of metals supported on
290 cheaper materials significantly increase fluoride removal.

291

292 **2.4.1.1 Monometallic based adsorbents**

293 The basic reason for using metallic compounds as adsorbents for fluoride removal is based on the
294 nature of these materials. Metallic elements have tendencies to give valence electrons and acquire positive
295 charge that attract negatively charged fluoride ions. The literature shows that the number of publications
296 on monometallic based adsorbents has increased in recent years. The adsorbents based on one metal are
297 relatively few: about 15 different metals have been used for preparing adsorbents for multiple
298 applications. One of the reasons is that many metals have not been used due to their toxicity.

299 From the first row of the periodic table (lithium, sodium, potassium, rubidium, cesium and
300 francium), lithium is the only metal that has been studied to remove fluoride, but has not been reported as
301 the principal element in the adsorbent, due to its relative high cost. The rest of alkali elements are
302 excluded for the purpose of fluoride removal from water as adsorbents. Sodium could be used to remove
303 fluoride via precipitation. On the other hand, alkali metals have the lowest electronegativity that results in
304 a high affinity to form bonds of covalent predominance. With regard to alkali, the most studied earth
305 metals are calcium and magnesium, which are the most abundant elements in earth's crust.

306 Islam and Patel [54] proposed that among various technologies, fluoride adsorption by using quick
307 lime appeared to be an interesting process. The use of quick lime as adsorbent to remove fluoride has not
308 been clarified, so this study was directed to understanding the adsorption process in a better way. The

309 inconvenience of this adsorbent is that results in chemisorption along with precipitation of fluoride.
310 Removal efficiency was found to be maximum when the initial fluoride concentration was high (>10 mg
311 L^{-1}). Therefore, the removal of fluoride using quick lime cannot be used for domestic purpose, since it
312 cannot bring fluoride concentration within permissible limit, and also increases the pH of the treated
313 water. Nath and Dutta [55] reported acid-enhanced limestone defluoridation in a column reactor. Ca^{2+}
314 ions, formed due to dissolution of limestone by oxalic acid, precipitate calcium fluoride along with
315 precipitation of calcium oxalate. A good fluoride removal ability, low residual oxalate, acceptable final
316 pH, low-cost and the simplicity of the process make the acid-enhanced limestone defluoridation process
317 with oxalic acid a potential method for defluoridation of groundwater. There are some other works where
318 the acid used is HCl, H_2SO_4 , HNO_3 , acetic acid or citric acid. When using strong acids, the remains in the
319 water are Cl^- , SO_4^{2-} and NO_3^- which are undesirable, while acetic and citric acid permit the enhancement
320 of fluoride removal. The tests with oxalic acid were in search for a more suitable acid keeping in mind that
321 being a stronger acid it should increase the concentration of Ca^{2+} . Moreover, very little oxalate should
322 remain in the treated water due to low solubility of calcium oxalate and high concentration of calcium ions
323 produced in the column. They concluded that the precipitation process is rapid whereas the adsorption is
324 slow and continues beyond 6 h. The adsorption is significant with fresh limestone but decreases with
325 repeated use of the limestone.

326 Another mineral of calcium used for fluoride removal is hydroxyapatite. Badillo-Almaraz et al., [56]
327 reported the use of commercial synthetic hydroxyapatite BIO-RAD and the best physicochemical
328 condition for removing the biggest quantity of fluoride present in drinking water. It is reported that the
329 retention of fluoride in the synthetic hydroxyapatite BIO-RAD diminishes notably as the pH rises.
330 Another study by Gao et al., [57] reported an interesting article named size-dependent defluoridation
331 properties of synthetic hydroxyapatite, where the results showed that the better performances in fluoride
332 removal were obtained with the smaller particle size and the efficiency was better at a low pH. On the
333 other hand, Poinern et al., [58] combined ultrasonic and microwave processes to produce nanoparticles of
334 hydroxyapatite, which allowed to control the size and morphology varying the experimental conditions
335 that regulate the particle nucleation and growth. The particles that were produced had a relatively low
336 fluoride adsorption capacity compared with some materials related to the precipitation process such as
337 quick lime, but these have the advantage that the equilibrium pH was 6.6, meaning that it would not be
338 necessary to readjust pH in water for human consumption. Moreover, Wang et al., [59] worked with
339 nanoparticles of hydroxyapatite and added low molecular-weight organic acids to improve fluoride
340 removal. They found that the acids formed new active sites for fluoride adsorption at low pH where acids
341 present a protonated state, and these organic acid anions could be exchanged with fluoride on the surface
342 of hydroxyapatite nanoparticles.

343 Regarding other monometallic-based adsorbents, Nagappa and Chandrappa [60] synthesized
344 mesoporous and nanocrystalline oxide manganese based adsorbents. These were prepared through
345 combustion route and the comparative study for fluoride removal capacity (in standard fluoride solution
346 10 ppm) showed an adsorption uptake of 97%, while the regenerated material reduced the uptake to 76%.
347 Maliyekkal et al., [61] also used synthesized MgO nanoparticles, but employed a cheaper synthesis
348 method than combustion with similar results in fluoride adsorption capacity. It was also reported that
349 phosphate ions affect the fluoride removal. With respect to the methods of synthesis of magnesium oxides,
350 Sasaki et al., [62] found that sorption of fluoride increased when the adsorbent was synthesized at
351 calcination temperatures that are lower than 873 K for 1h. The authors also reported that the process
352 involved co-precipitation of F⁻ with magnesium hydroxide.

353 In addition, the interest of rare earth metals like adsorbents came from the particular properties that
354 most of them exhibit, like multivalence behavior and the selectivity towards fluoride ions. Scandium and
355 yttrium elements behave more like rare earth metals than transitional ones, and since these are extracted
356 from minerals of rare earth metals they could be considered herein. Lanthanum has been studied to
357 remove fluoride from water, for instance, Na and Park [63] used lanthanum hydroxide which showed a
358 defluoridation capacity of 242.2 mg g⁻¹ at pH 7.5, and 24.8 mg g⁻¹ at pH 10. This material presented a
359 sorption energy close to chemical sorption, and the regeneration percentage was 24.9 and 89.7% for 0.1 M
360 NaOH and 2.0 M NaOH solutions, respectively. Rao and Karthikeyan [64] also studied the use of
361 lanthanum oxide for fluoride removal and reported that the sorption capacity ranges from 0.5 to 2.5 mg g⁻¹
362 ¹, depending upon initial concentration and a higher sorption capacity was accomplished at low pH values.
363 The energy of sorbent-sorbate bonding was found to be strong, which indicated a chemisorption process;
364 and alum was a more effective regenerant than HCl and NaOH.

365 Transition metals have much more interest for fluoride removal by adsorption than alkaline and
366 alkaline earth metals, because of their multivalent behavior and more “places” for the fluoride ion to
367 interact. The transferring electron interactions between these metals and fluoride ions are slightly weak
368 due to the higher electronegativity than alkaline and alkaline earth metals (with the exceptions of Mg and
369 Be) that tend to precipitate fluoride.

370 The elements mainly used for water treatment are iron, zirconium, titanium and manganese. More
371 than half of the reported studies related to monometallic compounds to remove fluoride use iron
372 compounds. Tang et al., [65] used goethite to simultaneously adsorb arsenic and fluoride, being less
373 favorable for fluoride. Granular ferric hydroxide was studied by Kumar et al., 2009 [66] and Tang et al.
374 [67]. Both coincided that certain anions reduce the fluoride removal in the next order H₂PO₄⁻ >HCO₃⁻
375 >SO₄²⁻. The first study found that the maximum fluoride removal was 7.0 mg g⁻¹ at 25°C and optimal pH
376 range between 4 and 8. The study of Tang et al., (2009) indicated that maximum fluoride adsorption was

377 achieved between pH 3 and 6.5, whereas the XPS results showed an inner-sphere complexation when
378 fluoride was adsorbed by iron in the granular hydroxide. Iron oxide nanomaterials were studied by
379 Mohapatra et al., [68] and found that this material, composed of different phases of iron oxides, had the
380 best adsorption at pH of 5.75 and that it was severely affected by sulfate and chloride anions. Zirconium
381 adsorbent in form of zirconium oxide showed a maximum fluoride adsorption capacity of 68 mg g^{-1} at pH
382 7, and it was concluded that hydrous zirconium oxide was superior to most Zr-containing adsorbents (Dou
383 et al. [69]). Moreover, Swain et al., [70] studied meso-structured zirconium phosphate and reported a
384 maximum adsorption of fluoride at pH 6. Although the process showed bonding energy related to ion
385 exchange, the material was used and regenerated up to five times.

386 Titanium dioxide has also been studied to remove fluoride, such is the case of Babaeivelni and
387 Khodadoust [9] who reported a maximum fluoride adsorption at a pH range of 2-5. It was also reported
388 that the presence of bicarbonate ion has a negative effect on fluoride uptake, but the selectivity of the
389 material was for fluoride over bicarbonate, sulfate and calcium ions. Wajima et al., [71] reported another
390 adsorbent for fluoride removal, titanium oxysulfate ($\text{TiOSO}_4 \cdot x\text{H}_2\text{O}$), which showed a maximum fluoride
391 adsorption at pH 3.

392 The *p*-block of the periodic table contains the elements Al, Ga, In, Sn, Tl, Pb and Bi. From these, Al,
393 Sn and Bi have been reported as adsorbents for fluoride contained in aqueous solutions. Historically
394 aluminum compounds are the best typical helper material in removal of contaminants from water and have
395 been extensively studied. The research for defluoridation with alumina (Al_2O_3) shows different kinds of
396 compounds which include different treatments to give it specific characteristics. Gong et al., [72] worked
397 with five types of alumina that were poorly crystallized and their anion exchange capacity and point of
398 zero charge varied for each one. Besides, acidic alumina exhibited higher ion exchange capacity with a
399 more positively charged surface and better defluoridation performance (higher adsorption capacity and
400 quicker removal of fluoride) than basic alumina. According to Goswami and Purkait [73], acidic alumina
401 followed the Langmuir model with an adsorption capacity of 8.4 mg g^{-1} and 94% of fluoride adsorbed at
402 pH 4.4. There are other kinds of alumina used for defluoridation processes, like one reported by Kamble et
403 al., [74] who used alumina of alkoxide, which is a gamma alumina that contains a small amount of Fe_2O_3 ,
404 SiO_2 and has activated carbon in its pores. Kumar et al., [75] worked with nano-alumina, and the
405 maximum fluoride sorption capacity reported was 14.0 mg g^{-1} at 25°C and pH 6.15. Liu et al., [76] and
406 Mulugeta et al., [77] have also studied alumina hydroxides to remove fluoride. According to Liu et al.,
407 [76], the maximum fluoride adsorption capacity was 110 mg g^{-1} in a pH range from 5.0 to 7.2, where the
408 characteristics of low particle diameter, high surface area, and surface reactivity of the amorphous
409 $\text{Al}_2\text{O}_3 \cdot x\text{H}_2\text{O}$ enable its high removal. The study presented by Mulugeta et al., [77] involved an adsorbent
410 based of aluminum hydroxide with 90% of $\text{Al}(\text{OH})_2 \cdot 8(\text{SO}_4)_{0.1}$ and 10.7% of aluminum sulfate and 10% of

411 sodium sulfate with impurities. The fluoride adsorption capacity (for continuous packed column
412 experiments at a flow rate of 100 empty bed volumes per day) was $26.2 \text{ mg F}^- \text{ g}^{-1}$. Additionally, Wang et
413 al., [78] concluded that nano- AlOOH possesses a maximum fluoride removal of $3.2 \times 10^{-3} \text{ mg g}^{-1}$, which is
414 comparable with the activated alumina, and has a maximum adsorption around pH 7. On the other hand,
415 Srivastav et al., [79] synthesized three forms of bismuth trioxide (Bi_2O_3) that were examined for
416 defluoridation of aqueous solutions. Those three additional bismuth hydro(oxides) (HBOs) were
417 synthesized from Bi_2O_3 , HCl and NaOH. The highest removal percentage presented in this work for those
418 materials was $\sim 65\%$ at 10 mg/L of initial fluoride concentration, while commercially available Bi_2O_3
419 powder removed approximately only 6% of fluoride. Table 2 shows the comparison of some monometallic
420 adsorbents and their performance for fluoride removal from water.

421

422 2.4.1.2 Bimetallic based adsorbents

423 In an effort to improve the fluoride adsorption capacity of single metal oxides, researchers have
424 developed bimetallic materials.

425 To enhance the alumina efficacy of fluoride removal, Liu et al., [80] studied the removal of this anion
426 using an Al-based material modified with Ce, Ti, La or Zr. The hybrid Al-La and Al-Zr increased their
427 adsorption capacity around 6.6 and 33%, respectively. Al-Ce possessed the highest adsorption capacity
428 (62 mg g^{-1}) with a Ce/Al molar ratio of 1:4, at pH 6 and 25°C . The preparation of the hybrid adsorbent
429 Ce-Al by co-precipitation with NaOH and a drying temperature of 80°C , allowed the formation of
430 nanoparticles. SEM and XRD results showed that the bimetallic adsorbent possessed an amorphous
431 structure with some aggregated nanoparticles. The point of zero charge at pH 9.6 showed that fluoride is
432 attracted by electrostatic interactions with $-\text{OH}$ exchange from the adsorbent surface. On the other hand,
433 Maliyekkal et al., [81] modified alumina with manganese oxide to prepare a Mn-Al adsorbent, and applied
434 it to defluoridation of drinking water. The optimal pH range for fluoride removal was 4-7, and the
435 maximum adsorption capacity reached with this adsorbent was 2.65 times higher than activated alumina
436 (2.851 mg g^{-1}). Moreover, the adsorption kinetics demonstrated that the manganese-oxide-coated alumina
437 was faster than activated alumina, which can be regenerated with 2.5% NaOH.

438 On the other hand, Tripathy and Raichur [82] also studied the effect of manganese dioxide coating on
439 activated alumina in the removal of fluoride. The authors found that the maximum adsorption capacity
440 reported by the Langmuir model was 0.16 mg g^{-1} , and the kinetic studies revealed that the adsorption
441 followed second-order rate kinetics, up to 0.2 mg L^{-1} , at pH 7 in 3 h and at 25°C . In this case, the fluoride
442 adsorption was attributed to physical adsorption.

443 Bansiwala et al., [83] modified mesoporous alumina with copper oxide to improve fluoride removal
444 from water. The adsorption capacity of the Cu-Al material obtained from the Langmuir model was 7.22

445 mg g^{-1} . The enhancement in the fluoride adsorption capacity was attributed to the increase in zeta potential
446 to more positive values. A decrease in sorption capacities was reported at pH above 8, and might be due to
447 the presence of OH^- ions that compete for the same adsorption sites. No leaching of copper occurred when
448 fluoride was adsorbed by the bimetallic material.

449 Following the co-precipitation methodology, Deng et al., [84] developed a Mn-Ce adsorbent. The
450 highest adsorption capacity was achieved at a Ce/Mn ratio of 1:1, at pH 6 and 25°C . In equilibrium
451 concentrations of 1 mg L^{-1} , the sorption capacity was 79.5 mg g^{-1} for the powder adsorbent and 45.5 mg g^{-1}
452 for the granular one. Furthermore, kinetics studies showed that the adsorption process took place in the
453 first hour, when the granular form of the adsorbent required 3 h to reach equilibrium, while the powder
454 accomplished it at 8 h.

455 Fe-Ti, another bimetallic oxide, was studied for water defluoridation by Lin et al. [85]. The optimized
456 Fe-Ti ratio was 2:1 with an adsorption capacity of 29.85 mg g^{-1} at 25°C . It was found that the hydroxyl
457 groups and Fe-O-Ti bonds on the adsorbent surface which provided active sites for adsorption: a Fe-O-F
458 bond is formed after F^- removal. Biswas et al., [86] incorporated Sn(IV) to iron(III) oxide, and the
459 maximum fluoride adsorption capacity was 10.50 mg g^{-1} in a pH range 5.0-7.5. This trend was presumably
460 due to the neutral or near neutral surface of the solid. The hybrid adsorbent can be regenerated up to a
461 level of 75 % with a bicarbonate solution, at pH 13. Previously, the same group developed a crystalline
462 and hydrous Fe(III)-Zr(IV) hybrid oxide for fluoride removal [87]. The optimum Fe/Zr ratio was 9:1, and
463 the pH range for F^- uptake was between 4.0 and 7.0. The pH_{ZPC} determined for the oxide was 7.1-7.2, and
464 the maximum adsorption capacity was 7.51 mg g^{-1} , at 20°C and pH 6.8. The kinetic data obtained for
465 fluoride removal described both the pseudo-first and the reversible first order equations. The kinetics also
466 demonstrated that the fluoride adsorption took place with a boundary layer diffusion. The external mass
467 transport with intra-particle diffusion phenomena governed the rate, limiting the process. Duo et al., [88]
468 developed another Zr-Fe adsorbent using an extrusion method that was composed of amorphous and nano-
469 scale oxide particles. The optimum Zr/Fe ratio was around 2.3, and the adsorption capacity reached with
470 this material was 9.80 mg g^{-1} under an equilibrium concentration of 10 mg L^{-1} at pH 7. Moreover, it had an
471 excellent mechanical stability and high crushing strength. The fluoride adsorption followed a pseudo-
472 second-order kinetics, and the presences of Cl^- , NO_3^- and SiO_4^{4-} did not inhibit the fluoride uptake, except
473 for HCO_3^- , PO_4^{3-} and AsO_4^{3-} . The authors tested the granular bimetallic adsorbent in columns using real
474 water and the results showed that it has high potential for fluoride removal.

475 Ti-Ce and Ti-La were prepared by Zhijian et al., [89] to enhance the fluoride adsorption capacity, in
476 which the doping Ce and La oxides increased the points of zero charge in the zeta potentials of the hybrid
477 adsorbents. At their points of zero charge, Ti-La and Ti-Ce ($\text{pH}_{\text{ZPC}} = 6.8$ and 6.2) adsorbed 18.7 and 22.6
478 mg g^{-1} , respectively, at a fluoride initial concentration of 10 mg L^{-1} . The sorption equilibrium was

479 achieved in 4 h where the pseudo-second order model described the sorption kinetics, besides, the
480 nonspecific electrostatic attraction and the specific anion exchange with hydroxyl groups were mainly
481 responsible for fluoride adsorption in the bimetallic adsorbents.

482 An iron-doped titanium oxide adsorbent was developed by Lin et al., [90]. This adsorbent had a
483 maximum fluoride adsorption capacity of 53.22 mg g^{-1} at pH 7 and $25 \text{ }^\circ\text{C}$, obtained by fitting the
484 experimental data with the Langmuir isotherm model. The adsorption of fluoride followed a second-order
485 kinetic. The authors prepared the adsorbent with an initial feed Fe/Ti molar ratio of 1, but a 0.35 molar
486 ratio was used during the optimization because the Ti ions precipitated faster and earlier than Fe ions
487 during the titration procedure used. It was found that the Fe doped into Ti oxide promoted the formation of
488 active hydroxyl groups on the adsorbent surface, and it increased the fluoride adsorption capacity. The
489 difference between the previous work by the same research group [85] and this study is that the feed molar
490 ratio of Fe/Ti and the pH were lower, and the washed process included just water instead of ethanol. Thus,
491 the differences in the synthesis process gave the iron-doped titanium oxide adsorbent a higher adsorption
492 capacity than Fe-Ti bimetallic oxide.

493 Following the mixed oxides, Biswas et al., [91] synthesized an iron(III)-aluminum(III) adsorbent for
494 fluoride removal from water. The results demonstrated that the optimum Fe/Al ratio was 1, and the
495 maximum adsorption capacity was 17.73 mg g^{-1} at pH 6.9, and $28 \text{ }^\circ\text{C}$. The authors established that this
496 mixed oxides could be a better adsorbent than either of the pure oxides. The equilibrium data were fitted
497 reasonably with the Langmuir and Redlich-Peterson models, and the equilibrium was reached in 1.5 h.
498 Moreover, the pseudo-second-order model described the adsorption kinetics, and the adsorption rate was
499 controlled by multistage diffusion.

500 Iron has also been used as an active agent in nanotechnology and this nanosized form has been
501 studied for defluoridation of water since several years ago. For instance, a material composed by
502 aluminum oxide embedded with Fe_2O_3 nanoparticles ($\text{Fe}_2\text{O}_3@\text{Al}(\text{OH})_3$) was prepared by Zhao et al., for
503 fluoride removal from aqueous solutions [92]. The adsorbent, in the range of 240-340 nm, presented
504 magnetic properties which can be an advantage for the easy separation from sample solutions by the
505 application of an external magnetic field. The optimal ratio $\text{Fe}_2\text{O}_3/\text{Al}(\text{OH})_3$ was 2:5, and the adsorption
506 capacity calculated by the Langmuir model was 88.49 mg g^{-1} at pH 6.5 and 25°C . The authors reported a
507 residual fluoride concentration of 0.3 mg L^{-1} when using $\text{Fe}_2\text{O}_3@\text{Al}(\text{OH})_3$ nanoparticles, with an initial
508 concentration of 20 mg L^{-1} , which met the standard of the World Health Organization (WHO) for safe
509 drinking water quality. Recently, Chai et al., [93] also developed sulfate-doped $\text{Fe}_2\text{O}_3/\text{Al}(\text{OH})_3$ magnetic
510 nanoparticles for fluoride removal from water. The authors reported a maximum fluoride adsorption
511 capacity of 70.4 mg g^{-1} at pH 7 and 25°C , where the fluoride sorption process can be achieved within 20
512 min with a 90% of F^- removal. SO_4^{2-} was released steadily from the nanoparticles with simultaneous

513 fluoride adsorption, indicating that an anion exchange mechanism took place during the fluoride removal.
514 The difference between this research and that conducted by Zhao et al., [92] is that the pH range for
515 fluoride adsorption was from 4.0 to 10.0, indicating the applicability of this developed nanoadsorbent for
516 water defluoridation.

517 The rare earth oxides occur as a mixture of various oxides, Raichur et al., [52] used these elements as
518 mixed rare earth oxides to remove fluoride from aqueous solutions. The chemical material composition
519 was a mixture of La_2O_3 (44%), CeO_2 (2%), Pr_6O_{11} (10.5%), Nd_2O_3 (36.5%), Sm_2O_3 (5%), among others in
520 trace amounts. The maximum fluoride adsorption capacity was 196.08 mg g^{-1} at pH 6.5 and 29°C , where
521 most of the adsorption took place in the first 10 min. The adsorption followed the Langmuir isotherm
522 model and it was found that sulfate and nitrate, up to 100 mg L^{-1} , did not greatly affect the fluoride uptake.
523 Adsorption studies demonstrated that fluoride can be desorbed at pH 12. However, the adsorption
524 efficiency decreased from 98 to 91% after the first regeneration.

525 Several layered double hydroxides (LDH) have been developed in order to make efficient fluoride
526 removal from water supplies. These mixtures are a family of lamellar compounds containing anions in the
527 interlayer space and have been recently focused on the synthesis of new hybrid materials for fluoride
528 removal from water. A recent study carried out by Kim et al., [94] demonstrated that the removal of high
529 fluoride concentrations by Mg/Al layered double hydroxides can be useful. Batch experiments
530 demonstrated that the optimal adsorbent was performed calcinating the Mg/Al LDH at 700°C , while the
531 X-ray analyses indicated a chemical composition of mixed metal oxides ($\text{Al}_8\text{O}_3\text{N}_6 + \text{Mg}_{0.44}\text{Al}_{0.55}$) and
532 magnesium oxide (MgO), respectively. Batch experiments showed that the fluoride sorption capacity was
533 1.7-2.9 times greater than Mg/Al calcined at a temperature less to 300°C , and the adsorption capacity was
534 91.4 mg g^{-1} . The kinetic data showed that the fluoride sorption arrived at equilibrium after 12 h. Moreover,
535 fluoride sorption decreased considerably in the presences of anions such as phosphate, sulfate and
536 carbonate.

537 Following the modification of adsorbents that contain Magnesium, Kang et al., [95] evaluated the
538 calcinated Mg/Fe layered double hydroxide (Mg/Fe-CLDH) as a material for fluoride and arsenate
539 removal from aqueous solutions. The adsorbent was synthesized by a co-precipitation method and the
540 optimal Mg/Fe ratio was 5, calcinated at 400°C , and the maximum adsorption capacity reached with this
541 material was 50.91 mg g^{-1} at pH 7. Data of equilibrium experiments were fitted by the Langmuir isotherm
542 model and pseudo-second order kinetic. The fluoride adsorption mechanism involved surface adsorption,
543 ion exchange interaction and the original layered double hydroxide (LDH) structure was reconstructed by
544 rehydration of mixed metal oxides and the intercalation of F ions into the interlayer region.

545 MgAl-CO_3 was developed by Luv et al., [96] to treat high fluoride concentration solutions (5-2500
546 mg L^{-1}). The adsorbent was prepared by a co-precipitation method as well, and the maximum adsorption

547 capacity of this LDH containing carbonate, where the data was fitted with the Langmuir-Freundlich
548 model, was 319.8 mg g⁻¹ at pH 6 and 30°C. The kinetic experiments showed that the fluoride adsorption
549 involves a rapid first order step and a slow second order step, and suggested that the second step was
550 controlled by diffusion. It was found that the fluoride removal decreased in presence of other anions in the
551 order of HCO₃⁻>Cl⁻>H₂PO₄⁻>SO₄²⁻, and the interlayer CO₃²⁻ of the LDH can be partially removed under
552 acidic conditions, with concomitant incorporation of fluoride in the interlayer galleries of the LDH's.

553 Batistella et al., [97] also tested MgAl containing CO₃²⁻ layered double hydroxide activated in acidic
554 conditions like HCl and HCOOH as reducing and complexing agents, respectively. The adsorption assays
555 showed that an enhancement in adsorption was verified at pH 3.5 and a temperature of 50 °C. The high
556 adsorption capacity reached with these conditions was 303.54 mg g⁻¹ within 10 min of contact time and
557 0.19 M HCOOH, which was slightly higher than what was reported previously [91].

558 Recently, Zhang et al., [98] tested a lamellar compound named CeO₂/Mg-Fe layered double
559 hydroxide composite for fluoride removal from water. In order to improve the fluoride removal efficiency,
560 non-thermal plasma (NTP) was used to modify the surface of these composites. The optimum Ce/Fe mol
561 ratio was 3/5 at 420 °C. The experimental results indicated that the adsorption was 52.4 mg g⁻¹ at pH 6-7
562 and 25 °C. The kinetic adsorption data was found to fit the pseudo-second order model, while the
563 equilibrium data was described by the Langmuir model. Also, the same research group developed another
564 layered double oxide composed (Li-Al-LDH) by a co-precipitation method [99]. The results indicated that
565 the maximum adsorption capacity reached with this adsorbent increased from 34.77 to 42.43 mg g⁻¹ as the
566 temperature increased from 10 to 40 °C, at pH 7. Besides, the adsorption kinetics of fluoride were
567 represented by the pseudo-second-order model and the experimental data were fitted by the Freundlich
568 isotherm model. It was also stated that from the kinetics analysis, chemisorption may be involved in the
569 adsorption process and can be inferred that an ion-exchange was implicated in a second adsorption stage.

570

571 **2.4.1.3 Trimetallic based adsorbents**

572 It has been presumed that multimetal mixed oxides may be good for filtering materials and for
573 scavenging high fluoride concentrations from contaminated water. Furthermore, it has been assumed that
574 multimetal mixed oxides may be the natural key material in scavenging fluoride from the fluoride-rich
575 percolated water [100].

576 In this context, Wu et al., [101] used a Fe-Al-Ce trimetal oxide in order to improve the adsorption
577 capacity of the Fe-Ce bimetal oxide. The results of their study show that the maximum fluoride removal
578 (95%) was achieved with an adsorbent calcined at 300 °C, achieving a fluoride adsorption capacity of 178
579 mg g⁻¹ at pH 7. The one-site and two-site Langmuir isotherm models were applied to fit the isotherm. The
580 experimental data were better fitted by the two-site Langmuir isotherm (R² = 0.992 and Q_{max} = 229 mg

581 g^{-1}), suggesting that there might exist two adsorption sites with different adsorption energies on the
582 adsorbent surface. The optimum pH for fluoride uptake was 6.0-6.5. However, the adsorbent also showed
583 a high adsorption capacity over a relatively wide pH range of 5.5-7.0, where the pH_{ZPC} of this adsorbent
584 was 7.5. The adsorption kinetic constant values of the first order rate (k) was determined as 0.002 and
585 0.0029 min^{-1} , respectively; and for concentrations of 10 mg L^{-1} and 50 mg L^{-1} the correlation coefficients
586 (r^2) were 0.978 and 0.982, respectively. Adsorption fluoride was partially inhibited by high concentrations
587 of phosphate or arsenate, and was not affected by the presence of chloride, sulfate, or nitrate. Desorption
588 results and column experiments further indicated the practicality of trimetal oxide Fe-Al-Ce to remove
589 fluoride for water.

590 The same group, Wu et al., [102], reported that increasing the initial fluoride concentration, the zeta
591 potential becomes more negative in the range of pH 4-10. To elucidate the fluoride adsorption mechanism
592 by Fe-Al-Ce, XPS and ^{19}F Mass-NMR were used in combination to identify the adsorption of F^- on Al-
593 Fe-Ce. They found a ligand exchange relationship between hydroxyl groups and metal-ions F^- . -OH
594 groups had contributed to adsorption of F^- , and although the Fe-Al-Ce contains a low proportion of Ce,
595 Ce-OH was the preferred site for adsorption at low loads of F^- . Al-F became the most abundant kind of
596 complex at higher load, which could be related to the high molar ratio of Al in the adsorbent. $\text{Al}_3\text{-F}$, $\text{Ce}_x\text{-}$
597 $\text{F}_y\text{-F}_y$ and $\text{Al}_3\text{Fe}_x\text{-F}$ were identified as fluorinated species after the adsorption process.

598 On the other hand, Biswas et al., [103] studied the fluoride removal efficiency of trimetal mixed
599 oxide (HIACMO) synthetic hydrated iron(III)-aluminum(III)-chromium(III) from an aqueous solution.
600 The HIACMO was synthesized by a simple chemical precipitation method. The HIACMO optimal pH for
601 fluoride adsorption was observed in a range of 4.0-7.0. The time required to reach the equilibrium was 1.5
602 h, and the kinetic data followed the equation of pseudo-second order. Equilibrium data were described by
603 the Langmuir isotherm model, and the maximum adsorption capacity reported was 31.8 mg g^{-1} .

604 Furthermore, Raichur and Basu [52] studied the efficacy of mixed rare earth oxides in the fluoride
605 adsorption synthetic solutions. Likewise, they studied the adsorption kinetics, the pH effect, the initial
606 fluoride concentration, the adsorbent dose and the presence of other anions in the fluoride adsorption
607 efficiency. The characterization results showed that the adsorbent's particle size was of $4.34 \mu\text{m}$, which
608 had a surface area of $6.75 \text{ m}^2 \text{ g}^{-1}$. The adsorption kinetics results demonstrated that during the first 5
609 minutes, the higher amount of fluoride was adsorbed. They found that the adsorption capacity was 12 mg
610 g^{-1} . Also, a dose of 8 g L^{-1} of adsorbent (at pH 6.5 and fluoride concentration of 50 mg L^{-1}) gave 98.5% of
611 fluoride elimination. The maximum fluoride adsorption was held in the range of 6 to 6.5 with an
612 adsorption capacity of 12.5 mg g^{-1} , which corresponded to the Langmuir model. Anions such as nitrate
613 and sulfate affected fluoride uptake. They also reported that desorption of fluoride occurs at pH 12 and

614 that the adsorption efficiency decreased from 98 to 91% after the first regeneration. Table 3 shows the
615 adsorption capacity of selected multimetallic adsorbents for fluoride removal from aqueous solutions.

616

617 **2.4.2 Metal-impregnated based adsorbents**

618 **2.4.2.1 Carbon based adsorbents**

619 Although carbon based adsorbents poorly remove fluoride from water, their carbonaceous matrix
620 provides a high surface area and inhibits metal sintering in their pore structure. These properties allow
621 modifying the carbons surface with metals to increase their fluoride adsorption capacity.

622 Cerium dispersed in carbon was reported by V. Sivasankar et al., [104]. This material was prepared
623 by a carbonization of ammonium cerium sulfate impregnated with starch. The maximum fluoride uptake
624 was determined to be 52 mg g^{-1} at a pH value of 8. Hernandez-Montoya et al., [105] also developed an
625 activated carbon by modifying nutshell with a calcium solution derived from an eggshell. The authors
626 reported an adsorption capacity of 2.3 mg g^{-1} at 30°C , and found that the calcium chemical species on the
627 carbon surface were more important than the carbon textural parameters in the fluoride adsorption process.
628 The presence of sulfate and hydrogencarbonate decreased the adsorption capacity, showing that both limit
629 the selectivity of Ca-impregnated activated carbon.

630 Another research group by Tchomgui-Kamga et al., [106] developed activated carbons that were
631 impregnated with 1M mixture of Al and Fe salts, followed by carbonization at temperatures between 500-
632 900°C . The optimum adsorbent was carbonized at 650°C . It was found that the maximum adsorption
633 capacity was 13.64 mg g^{-1} at 28°C , and more than 92% removal of fluoride was achieved within 24 h at
634 pH 7 with a 10 mg L^{-1} of F^- initial concentration. The kinetic data showed that the adsorption process
635 followed a pseudo-second order model at neutral pH, it was possible to find a residual amount of Al and
636 Fe of 0.67 and 1.8 mg L^{-1} , respectively. These materials showed the presence of crystallized CaCO_3 and
637 CaO. Despite this content, all the charcoals showed acidic surface properties and points of zero charge
638 (pH_{PZC}) values between 7.4–7.7. The fluoride removal was not modified by the presence of NO_3^- , SO_4^{2-}
639 and PO_4^{3-} , while HCO_3^- and Cl^- slightly affected the defluoridation capacity. Leyva et al., [48] also
640 synthesized aluminum-impregnated carbon with 3 to 5 times higher fluoride adsorption capacity. It was
641 reported by Ma et al., [107] that granular activated carbon (GAC) coated with manganese oxides like
642 MnO_2 and Mn_3O_4 improved the fluoride removal by at least three times. This material presented
643 amorphous characteristics and the predominant valence on manganese was 4.

644 Materials including zirconium are the most studied to remove fluoride from water. Janardhana et al.,
645 [108] investigated the potential of a zirconium-impregnated activated charcoal. This material showed a
646 fluoride adsorption capacity of 3–5 times higher than plain activated charcoal. Zirconium impregnated
647 coconut fiber charcoal (ZICFC) was developed by Sathish et al., [109] and showed a maximum fluoride

648 uptake followed by groundnut shell and coconut shell charcoals. Regeneration of ZICFC was conducted
649 by an elution of 0.02 M NaOH solution. Carbon nut shell carbon was also impregnated with zirconium by
650 Alagumuthu and Rajan [110] who found that the optimum conditions to remove fluoride from water (1.83
651 mg g^{-1}) were pH 7, particle size of 53 μm and room temperature (303K). This adsorbent could be
652 regenerated 96.2% with 2.5% sodium hydroxide in 180 min. Moreover, the equilibrium sorption data
653 agreed reasonably well with the Langmuir isotherm model, and the sorption dynamic study revealed that
654 the sorption process followed the pseudo-second-order equation; the sorption process was complex, both
655 at the boundary of liquid film and intra-particle diffusion contributed to the rate-determining step. On
656 the other hand, Li et al., [111] synthesized a manganese oxide coated graphene oxide that presented 8.34
657 times more fluoride removal than graphene oxide. The maximum adsorption capacity was 11.93 mg g^{-1}
658 and the optimum removal of fluoride occurred in a pH range of 5.5–6.7.

659 Our research group has tailored an activated carbon modified with Zr(IV) and oxalic acid [112], that
660 presented 3 times higher fluoride adsorption capacity (5.94 mg g^{-1}) than both Zr-impregnated coconut
661 fiber carbon [109] and Ca-impregnated nutshell carbons [106], at pH 7, $C_e = 40 \text{ mg L}^{-1}$ and 25°C. We also
662 found that without the presence of the organic acid, the adsorption capacity increased by only 32%, and
663 the kinetics studies revealed that the Zr-impregnated activated carbon removed 71% of the initial fluoride
664 concentration in the first 15 minutes, reaching equilibrium in 50 min. Table 4 shows the comparison of
665 some carbon based adsorbents and their performance for fluoride removal from water.

666

667 2.4.2.2 Biosorbents and natural materials (clays, zeolites, minerals, mud) modified with metals

668 Biosorbents normally refer to naturally occurring biomasses or spent biomasses that passively bind
669 to organic molecules or metal ions by a phenomenon commonly referred to as biosorption [113-115]. It
670 was reported in the literature that the presence of chemical functional groups such as hydroxyl, carbonyl,
671 carboxyl, sulfhydryl, thioether, sulfonate, amine amide, imidazole, phosphonate and phosphodiester
672 present on the biosorbents surface contribute to biosorption [115-116]. Applications of biosorbent/biomass
673 from various microbial sources, leaf-based adsorbents and water hyacinth have been reported by various
674 investigators [117-123]. Moreover, biosorbents have been modified with metal ions to improve their
675 natural adsorption capacity.

676 In this subject, Yao et al., [124] used neodymium-modified chitosan for defluoridation of water.
677 The treatment conditions were optimized at pH 7, 323 K and a particle size of 0.10 μm . The equilibrium
678 sorption data were also fitted reasonably well by the Langmuir isotherm model. The maximum
679 equilibrium sorption was 22.38 mg g^{-1} at 303 K. Sorption dynamic studies revealed that the sorption
680 process followed a pseudo-second-order equation; and showed that the sorption process was complex
681 where the boundary of liquid film and intra-particle diffusion contributed to the rate-determining step. The

682 used adsorbents were regenerated with 4 g L⁻¹ of NaOH during 24 h. Following this theme, Sundaram et
683 al., [125] used a bioinorganic composite named nano-hydroxyapatite/chitosan (n-HApC) composite which
684 could be employed for water defluoridation. It was observed that there was a slight enhancement in the
685 defluoridation capacity of n-HApC composite (1.56 mg g⁻¹) compared to nano-hydroxyapatite (n-HAp),
686 which showed a fluoride uptake of 1.29 mg F⁻ g⁻¹. Other contributions by Sundaram et al., [126-127]
687 reported that nano-hydroxyapatite/chitosan composites, showed an increase in fluoride adsorption capacity
688 from 1.29 mg g⁻¹ to 1.56 mg g⁻¹, and concluded that the use of chitosan is justified by its biocompatibility.

689 Jagtap et al., [128] also studied a modified chitosan-based adsorbent for defluoridation of water.
690 The authors showed that when keeping constant the adsorbent dose of 1 mg L⁻¹, pH 7.03, 150 rpm and a
691 contact time of 24 h, an increase of initial fluoride concentration decreased the percentage of removal of
692 fluoride, while the adsorption capacity increased (9 mg g⁻¹). This was attributed to the amount of fluoride
693 ions available for adsorption as the concentration increases. Another study that involved biopolymers is
694 that by Kamble et al., [129] who studied the applicability of chitin, chitosan and 20%-lanthanum
695 incorporated chitosan (20% La-chitosan) as adsorbents for fluoride removal from drinking water. The
696 effects of physico-chemical parameters such as pH, adsorbent dose, initial fluoride concentration and the
697 presence of interfering ions during the adsorption were studied. The authors observed that the maximum
698 fluoride uptake was 3.1 mg g⁻¹ at pH 6.7 and an adsorbent dose of 1.5 g L⁻¹. The equilibrium adsorption
699 data were fitted reasonably well with the Freundlich isotherm model, and the presence of chloride, sulfate,
700 carbonate and bicarbonate ions in drinking water greatly affected the fluoride uptake. These results
701 indicated that the anions compete with sorption of fluoride on 20% La-chitosan. The adsorption rate was
702 considered rapid, and the maximum fluoride uptake was attained within 20 min. Following with chitosan
703 as biosorbent, Bansiwala et al., [130] used lanthanum incorporated chitosan beads (LCB) to remove
704 fluoride from water. The equilibrium adsorption data was fitted by the Langmuir isotherm model and
705 showed a maximum fluoride adsorption capacity of 4.7 mg g⁻¹ at pH 5 with negligible lanthanum release.
706 Additionally, kinetic studies revealed that fluoride uptake was fast, and follows a pseudo-first-order
707 kinetics, whereas the presence of sulphate, nitrate and chloride marginally affected the removal efficiency,
708 however, drastic reduction in fluoride uptake was observed in the presence of carbonate and bicarbonate.
709 Thakre et al., [131] and Bansiwala et al., [130] agreed that the optimum loading of lanthanum was 10% and
710 that the maximum fluoride adsorption capacity of lanthanum incorporated in chitosan beds is 4.7 mg g⁻¹.
711 Chitosan flakes impregnated with lanthanum were studied by Jagtap et al., [132] in which the loading of
712 lanthanum was 20% and found a maximum adsorption capacity of 1.27 mg g⁻¹. They mentioned that the
713 advantage of using chitosan over other supports like cellulose, activated carbon and alumina is that
714 chitosan contains amino groups that have the ability to bind with the metal ions by forming complexes.

715 Following with modified chitosan for fluoride removal, Viswanathan and Meenakshi [133]
716 developed a chitosan doped with Fe and they found that the fluoride adsorption capacity rose from 0.052
717 to 4.23 mg F⁻ g⁻¹. In addition, the same group (Viswanathan and Meenakshi [134]) doped chitosan with
718 Zr(IV), as well as Liu et al., [136] who loaded Zr(IV) in carboxylated chitosan beads. The first authors
719 compared the defluoridation capacity of Zirconium modified chitosan (4.85 mg g⁻¹) with carboxylated
720 chitosan beads and raw chitosan beads which adsorbed 1.385 and 0.052 mg F⁻ g⁻¹, respectively. Liu et al.,
721 [135] synthesized a bio-based Zr(IV) impregnated dithiocarbamate modified chitosan bead material and
722 found a defluoridation capacity of about 4.58 mg F⁻ g⁻¹ at pH 7.0, 30 °C and 40 min. With respect to
723 impregnated chitosan with aluminum, Swain et al., [136] found that the percentage of fluoride adsorption
724 was 84% for the first cycle operating batch study, with an initial concentration of 10 mg L⁻¹, and had a
725 good desorption capacity of 92% at pH 12. Furthermore, Viswanathan and Meenakshi [137] developed an
726 alumina/chitosan composite for defluoridation and found an enhanced capacity of 3.81 mg g⁻¹ in
727 comparison with alumina and chitosan that showed an adsorption capacity of 1.56 and 52 mg g⁻¹,
728 respectively. Neodymium-modified chitosan was employed for defluoridation by Yao et al., [124] where
729 the maximum sorption equilibrium was between 11.41–22.38 mg g⁻¹, depending on the temperature (283–
730 323 K), pH (5–9), adsorbent dose (0.2–2.0 g L⁻¹), particle size (0.10–0.50 mm) and presence of co-anions
731 (NO₃⁻, Cl⁻ and SO₄²⁻). Moreover, the adsorbents could be regenerated in 24 h by 4 g L⁻¹ of sodium
732 hydroxide.

733 Some other biosorbents have also been evaluated to remove fluoride from water. Ramanaiah et al.,
734 [138] used waste fungus (*Pleurotus ostreatus* 1804 SP) and reported that the fluoride–fungal interaction fit
735 a pseudo-first-order rate equation. The amount of fluoride adsorbed per unit mass of fungus showed an
736 increasing trend up to 20 mg L⁻¹, and the experimental data fitted well the Langmuir's adsorption isotherm
737 model with an adsorption capacity of 1.27 mg g⁻¹ at pH 7 and 30 °C. Desorption was more evident in an
738 inorganic solution and distilled water. Besides, the effect of temperature on the degradation of the
739 fluoride-loaded biosorbent was also studied for its disposal ability. On the other hand, Mohan et al., [120]
740 employed algal *Spirogyra* 101, and showed its ability to remove fluoride from aqueous phase. Batch
741 sorption studies performed on the algal–fluoride system indicated an adsorption capacity of 1.272 mg g⁻¹,
742 which was more effective with a low pH (2 to 5). The initial high uptake of fluoride was attributed to
743 chemisorption interactions, and the fluoride–algal interactions were corroborated with the pseudo-first-
744 order rate equation.

745 Cellulose is the most abundant renewable biopolymer on earth, and has a low cost and is a
746 promising raw material to synthesize adsorbents for defluoridation of aqueous solutions. Yu et al., [139]
747 found that the agglomeration of nano-size hydroxyapatite (HA) can be avoided by using cellulose as a
748 template to disperse nano-size HA in the cellulose matrix. This adsorbent combines the advantages of

749 cellulose and HA for fluoride removal, moreover, the composite materials showed a higher adsorption
750 capacity than the nano-size HA. It was also reported that the residual fluoride concentration in drinking
751 water could meet the drinking water standard established by the World Health Organization (WHO) by
752 using more than 3 g L^{-1} of adsorbent in the initial fluoride concentration of 10 mg L^{-1} . Another composite,
753 Fe(III)-loaded ligand exchanged cotton cellulose adsorbent (Fe(III)LECCA), was synthesized by Zhao et
754 al., [140]. This matrix was selected for being an inexpensive and biodegradable carrier, and a macroporous
755 cellulose material with high surface area while Fe(III) was considered due to its strong affinity towards
756 fluoride anions, environmental safety and low cost. The adsorption followed a first-order rate reaction and
757 the adsorption capacity was 18.6 mg g^{-1} at $25 \text{ }^\circ\text{C}$. The leakage of Fe(III) from the adsorbent was just
758 below 0.3 mg L^{-1} due to the strong complex action between phosphonometry amino group of LECCA and
759 the chelating center Fe(III). On the other hand, in column experiments, with 20 mg L^{-1} influent fluoride at
760 26 BV h^{-1} flow rate under $25 \text{ }^\circ\text{C}$, the column gained 5.6 mg g^{-1} breakthrough adsorption capacity and
761 NaOH regeneration was effective in up to 8 adsorption-desorption cycles.

762 Among natural adsorbents, Suzuki et al., [141] and Xu et al., [142] developed a defluoridation
763 water-kaolinite-MgO system and magnesia-loaded fly ash cenospheres (MLC), constituted with silica and
764 alumina, respectively. The modified MgO was proposed with the final objective of evaluating the use of
765 commercial-grade MgO as a fluoride immobilization agent in soils. The studies of sorption with enough
766 MgO added to the water-kaolinite (soil model) system worked better for defluoridation and it was
767 considered as a reliable immobilizer for fluoride ions. Commercial-grade MgO had a fluoride adsorption
768 capacity of 64 mg g^{-1} at pH 11.5, and the fluoride adsorption mechanism was attributed to its
769 incorporation into the $\text{Mg}(\text{OH})_2$ by $-\text{OH}$ substitution. Furthermore, the dominant fluoride immobilization
770 agent for soils was kaolinite. In addition, a series of fluoride leaching tests showed that kaolinite without
771 MgO is vulnerable to an alkali attack, and the fluoride desorption from the contaminated kaolinite took
772 around 3-4 days. On the other hand, magnesia-loaded fly ash cenospheres [142] had a maximum fluoride
773 adsorption capacity of 6 mg g^{-1} at pH 3 and $45 \text{ }^\circ\text{C}$. The coexisting ions had a large impact
774 (phosphate>nitrate>sulfate) on the fluoride sorption on MLC, and the experimental data fitted well the
775 pseudo-second order kinetic model and followed the Langmuir isotherm.

776 Orange waste, and its modification with metal ions, has also been studied for water defluoridation.
777 For instance, Zr(IV) was loaded on a dried orange juice residue (Zr(IV)-DOJR) by Paudyal et al., [143].
778 The optimal parameter in the fixed bed column for Zr(IV)-DOJR that removed 13.9 mg g^{-1} were 14.3 mg
779 L^{-1} of influent fluoride concentration, 1.2 cm of bed depth and 2.55 ml min^{-1} of flow rate. The
780 breakthrough time was 50 min. , and the breakthrough curve model showed that Thomas and the Bed
781 Depth Service Time (BDST) models were in agreement. Furthermore, dilute alkali (0.1 NaOH) solution
782 was effective to desorb fluoride from the loaded column. The same authors [144] prepared an adsorbent

783 with rare earth metal ions and orange waste with a saponification reaction using lime for water
784 defluoridation. The maximum adsorption capacity for fluoride was reported at 0.60, 0.92, 1.06 and 1.22
785 mmol g⁻¹ for Sc (III), Ho (III), La (III) and Sm (III) loaded adsorbent, respectively. They concluded that
786 the La(III)- and Sm(III)- saponified orange juice residue (SOJR) had stronger interaction with fluoride
787 ions even with a trace concentration, suggesting that these materials can be employed as effective
788 adsorbents for the treatment of industrial effluents containing a trace concentration of fluoride ions.

789 Rice husk ashes and aerobic granules were also evaluated to remove fluoride from water, as reported
790 by Ganvir and Das [145] and Wang et al., [146], respectively. In the first study, the authors coated the
791 biosorbent with aluminum hydroxide and found a high fluoride adsorption capacity of 19 mg g⁻¹. On the
792 other hand, the aerobic granules, self-aggregation of microorganisms, were modified with Ce(III). Those
793 granules showed a fluoride adsorption capacity of 45.80 mg g⁻¹ at a neutral pH, that corresponded to an
794 increase of 359 % compared to the pristine aerobic granules. Also the highest adsorption capacity
795 occurred in the pH range of 3.0 to 5.0.

796 Alginate beads doped with Fe(III) or La(III) were studied by Sujana et al., [147] and Huo et al.,
797 [148], respectively. Hydrous ferric oxide doped alginate beads [149] worked better between pH 3.5 and 5,
798 although their adsorption capacity was significant (45-55%) around neutral pH. The beads were 0.8-0.9
799 mm size and contained 32-33 % Fe(III), and showed a specific surface area of 25.8 m² g⁻¹ and a pHPZC of
800 5.15. Modified beads showed a Langmuir F⁻ adsorption capacity of 8.9 mg g⁻¹ at pH 7 and the adsorption
801 kinetics were described by the pseudo-second order kinetic model followed by an intraparticle diffusion as
802 the rate-determining step. Moreover, lanthanum alginate beads [148] showed that the fluoride adsorption
803 isotherm was well fitted by the Langmuir model, and the maximum adsorption capacity was 197.2 mg g⁻¹
804 at pH 4. The amount of La(III) in the alginate beds was 25 % with a specific surface of 4.05 m² g⁻¹. Also,
805 the mechanism involved in fluoride adsorption by lanthanum alginate beads was an ion-exchange between
806 F⁻ and Cl⁻ or OH⁻. Another research group by Zhou et al., [149] reported that the La³⁺-impregnated cross-
807 linked gelatin exhibited the maximum adsorption capacity of 98.8 % with a pH range of 5-7 (21.28 mg g⁻¹),
808 while the adsorption followed a first-order reaction. Moreover, the adsorption capacity decreased to
809 82.3% after the adsorbent was regenerated three times with 1 M NaOH. Table 5 shows the adsorption
810 capacity of modified biosorbents and natural materials for fluoride removal from aqueous solutions.

811

812 2.4.2.2.1 Synthetic resins, ceramics and polymers

813 Chen et al., [150] developed an iron-impregnated granular ceramic for water defluoridation. This
814 material was prepared with Kanuma mud, zeolite and starch, with FeSO₄•7H₂O or Fe₂O₃. It was found that
815 the granular ceramic with FeSO₄ was more effective for fluoride removal than the one that contained
816 Fe₂O₃. The maximum fluoride adsorption on ceramic-FeSO₄ at pH 7 was 94.2 %, and the equilibrium data

817 was well fitted by both Langmuir and Freundlich models. Kinetics were governed by intraparticle
818 diffusion and followed a second-order kinetics model. The particle size was around 3-5 mm, which would
819 not block the sewer and could be easily separated from water. On the other hand, a hybrid sorbent of
820 Zr(IV)-ethylenediamine was synthesized by Swain et al., [151] where the combination of zirconium(IV)
821 and ethylenediamine reaction lead to the formation of a kind of gel material. The maximum fluoride
822 removal (37.03 mg g^{-1}) was performed at pH 7, while the adsorption process followed a pseudo-second
823 order kinetic model. The fluoride adsorption mechanism onto Zr(IV)-ethylenediamine adsorbent
824 suggested an ion exchange mechanism fluoride $-\text{OH}$ groups. Moreover, the presence of NO_3^- , Cl^- or SO_4^{2-}
825 did not have significant impact on fluoride removal.

826 Polystyrene has also been doped by Zr(IV), as reported by Samatya et al. [152]. This adsorbent
827 material had the higher fluoride adsorption capacity, 6.14 mg g^{-1} , between pH 2 and 4. The performance of
828 this adsorbent was also studied in packed columns, which showed an optimum fluoride breakthrough
829 capacity of 5.52 mg g^{-1} , with an elution efficiency of 83% by 0.1M NaOH.

830 The wetness impregnation-coprecipitation of a material containing silicon (SiMCM-41) with
831 Cerium (IV) oxide was studied by Xu et al., [153], who reported a fluoride adsorption capacity between 5-
832 $6 \text{ mmol F}^- \text{ g}^{-1}$ at 20°C and initial fluoride concentration of 2 mmol L^{-1} . Even thorium, a radioactive
833 chemical element, has been used to synthesize a hybrid thorium phosphate composite, Islam et al., [154]
834 that consisted of polycinnamamide thorium (IV) phosphate. The removal of fluoride by this composite
835 was 87.6% and the adsorption capacity, calculated from the Langmuir isotherm, was found to be 4.74 mg
836 g^{-1} . The authors explained that the main advantage of the polymeric composite resides in the possibility of
837 combining the physical properties of the constituents to obtain new structural or functional properties that
838 can be shaped into any desired form (beads, candles and membranes).

839 Lanthanum (III) is another element that has been loaded in polymeric matrices, Fang et al. [155].
840 These authors concluded that the different chemical composition and chemical structure of the polymer
841 matrix play the most important role in fluoride adsorption, and that the strongly acidic adsorbents are more
842 effective on fluoride removal in a neutral pH than weak acidic adsorbents, and finally that in the neutral
843 pH range of 4.5–8.0, the 200CT resin loaded with La would be the most appropriate adsorbent for small
844 amounts of fluoride existing in hot spring water.

845 Recently, Chen et al., [156] reported the development of a Fe-Al impregnated granular ceramic for
846 fluoride removal from an aqueous solution. It was found that the maximum adsorption capacity was 3.56
847 mg g^{-1} according to the Langmuir model, and the adsorption process was explained with the pseudo-
848 second-order and pore diffusion models. The authors found that more than 96% of F^- adsorption was
849 performed within 48 h from a 10 mg L^{-1} initial fluoride solution at pH 7. Also, the presence of CO_3^{2-} and
850 PO_4^{3-} significantly reduced the fluoride removal efficiency. Furthermore, Wu et al., [157] immobilized Fe-

851 Al-Ce on a porous matrix of polyvinyl alcohol (PVA) by crosslinking with boric acid. The 3-5 mm size-
852 granules gave high hydraulic conductivity in packed beds for the removal of fluoride from drinking water.
853 The trimetallic oxide and PVA were found to form chemical bonds, which made the oxide heavily loaded
854 in the porous structure of PVA. Moreover, the trimetallic oxide concentration was higher than the PVA
855 concentration (7.5%) which produced a higher adsorption capacity in the granules; achieving an
856 adsorption capacity of fluoride ions of 4.46 mg g^{-1} at pH 6.5, at an initial fluoride concentration of 19 mg
857 L^{-1} . Table 6 shows the fluoride adsorption capacity of some modified synthetic resins, ceramics and
858 polymers.

859

860 **3. Final remarks**

861 It is evident that the presence of fluoride in water supplies in many countries around the world is
862 still a problem to be solved. As shown in this review, different processes can be used to remove fluoride
863 from water. However, the adsorption process is generally considered more attractive because of its
864 effectiveness, convenience, ease of operation, simplicity of design, and for economic and environmental
865 reasons. Moreover, the improvement of different organic and inorganic adsorbents is progressing with the
866 support of nanotechnology and advanced characterization techniques. Metal
867 oxides/hydroxides/oxihydroxides and mixed metal oxides have shown a high potential to remove fluoride
868 from water, however, it is important to consider that the efficiency, selectivity, chemical and physical
869 stability, and cost are still drawbacks that have to be improved. Additionally, there is the need to validate
870 through adsorption-desorption cycles the use of the many adsorbent materials, reported in the literature, in
871 continuous systems at laboratory and pilot scale before these materials may be applied in water treatment
872 systems to meet the water regulations. Finally, it is evident that more research is needed to develop
873 adsorbent materials that provide suitable and economical solutions to remove fluoride from water,
874 especially for those communities in third world countries that do not have access to safe drinking water.

875

876 **4. Acknowledgments**

877 This work was financially supported by grants from CONACYT-Ciencia Basica (SEP-CB-2008-01-
878 105920 and SEP-CB-2014-237118). Litza H. Velazquez, Esmeralda Vences and Jose L. Flores would like
879 to thank CONACYT for receiving the scholarship. Finally, the authors thank Lucia Aldana N. for the
880 assistance in the English writing of this manuscript.

881

882 **5. References**

883 1. Gosh, A., Mukherjee, K., Gosh S.K., Saha B., 2013. Sources and toxicity of fluoride in the
884 environment, Res. Chem. Intermed. 39, 2881-2915.

- 885 2. Facts about global groundwater usage, compiled by the National Groundwater Association, USA,
886 <http://www.ngwa.org/Fundamentals/use/Documents/global-groundwater-use-fact-sheet.pdf>.
887 (Accessed on May 2015).
- 888 3. WHO, Guidelines for drinking water quality, 3rd ed., vol. 1, Recommendations. World Health
889 Organization, Geneva, 2004.
- 890 4. Ozsvath, D. L., 2009. Fluoride and environmental health: a review, *Rev. Environ. Sci. Technol.* 8,
891 59-79.
- 892 5. WHO, Guidelines for drinking water quality, 4th ed. World Health Organization, Geneva, 2011.
- 893 6. UNICEF, 1999. WaterFront, Fluoride in water: an overview, Programme Division, 13 pp. 11-14.
- 894 7. EPA, National Primary Water Regulations in EPA 40 CFR Parts 141-143. Environmental Protection
895 Agency, USA, 1991.
- 896 8. Onyango, M.S., Matsuda, H., 2006. Fluoride removal from water using adsorption technique, *Adv.*
897 *Fluorine Sci.* 2, 1-48.
- 898 9. Babaeivlni, K., Khodadoust, A.P., 2013. Adsorption of fluoride onto crystalline titanium dioxide:
899 Effect of pH, ionic strength, and co-existing ions. *J. Colloid Interface Sci*, 394, 419-427.
- 900 10. Mondal, P., Suja, G. 2015. A review on adsorbents used for defluoridation of drinking water, *Rev.*
901 *Environ. Sci. Biotechnol.*, 14, 195-210.
- 902 11. Tomar, V., Kumar, D., 2013. A critical study on efficiency of different materials for fluoride removal
903 from aqueous media, *Chem. Central J.* 7, 51-66.
- 904 12. Bhatnagar, A., Kumar, E., Sillanpaa, M., 2011. Fluoride removal from water by adsorption- a review,
905 *Chem Eng. J.* 171, 811-840.
- 906 13. Loganathan, P., Vigneswaran, S. Kandasamy J., Naidu, R., 2013. Defluoridation of drinking water
907 using adsorption processes, *J. Haz. Mat.* 248-249, 1-19.
- 908 14. Hao, O., Huang, C., 1986. Adsorption Characteristics of Fluoride onto Hydrous Alumina. *J. Environ.*
909 *Eng.* 112, 1054-1069.
- 910 15. Shen, F., Chen, X., Gao, P., Chen G., 2003. Electrochemical removal of fluoride ions from industrial
911 wastewater, *Chem. Eng. Sci.* 58, 987-993.
- 912 16. Mollah, M.Y.A., Schennach, R., Parga, J.R., Cocke, D.L., 2001. Electrocoagulation (EC) science and
913 applications, *J. Hazard. Mater.* 84, 29-41.
- 914 17. Chen, G.H., 2004. Electrochemical technologies in wastewater treatment, *Sep. Purif. Technol.* 38,
915 11-41.
- 916 18. Liu, R., Zhu, L., Gong, W., Lan, H., Liu, H., Qu, J., 2013. Effects of fluoride on coagulation
917 performance of aluminum chloride towards Kaolin suspension, *Colloids and Surfaces A:*
918 *Physicochem. Eng. Aspects* 421, 84-90.

- 919 19. Hu, C.Y., Lo, S.L., Kuan, W.H., 2005. Effects of the molar ratio of hydroxide and fluoride to Al(III)
920 on fluoride removal by coagulation and electrocoagulation, *J. Colloid Inter. Sci.* 283, 472–476.
- 921 20. Sujana, M.G., Thakur, R.S., Rao, S.B., 1998. Removal of Fluoride from Aqueous Solution by Using
922 Alum Sludge, *J. Colloid Inter. Sci.* 206, 94–101.
- 923 21. Zhu, J., Zhao, H., Ni, J., 2007. Fluoride distribution in electrocoagulation defluoridation process, *Sep.*
924 *Purif. Technol.* 56, 184–191.
- 925 22. Hu, C.Y., Lo, S.L., Kuan, W.H., 2007. Simulation the kinetics of fluoride removal by
926 electrocoagulation (EC) process using aluminum electrodes, *J. Haz. Mat.* 145, 180–185.
- 927 23. Gong, W.X., Qu, J.H., Liu, R.P., Lan, H.C., 2012. Effect of aluminum fluoride complexation on
928 fluoride removal by coagulation, *Colloids and Surfaces A: Physicochem. Eng. Aspects*, 395, 88–93.
- 929 24. Ayoob, S., Gupta, A.K., Bhat, V.T., 2008. A conceptual overview on sustainable technologies for the
930 defluoridation of drinking water, *Critical Rev. Environ. Sci. Technol.* 38, 401-470.
- 931 25. Arora, M., Maheshwari, R.C., Jain, S.K., Gupta, A., 2004. Use of membrane technology for potable
932 water production, *Desalination* 170, 105-112.
- 933 26. Ndiaye, P.I., Moulin, P., Dominguez, L., Millet, J.C., Charbit, F., 2005. Removal of fluoride from
934 electronic industrial effluent by RO membrane separation, *Desalination* 173, 25-32.
- 935 27. Nicolas, S., Guihard, L., Marchand, A., Bariou, B., Amrane, A., Mazighi, A., Mameri N., El
936 Midaoui, A., 2010. Defluoridation of backish northern Sahara groundwater-Activity product
937 calculations in order to optimize pretreatment before reverse osmosis, *Desalination* 256, 9-15.
- 938 28. Peinemann, K.V., Nunes, S. P., 2011. *Membrane Technology, Volume 1: Membranes for Life*
939 *Sciences.* John Wiley & Sons, pp. 157.
- 940 29. Hichour, M., Persin, F., Sandeaux, J., Gaavach, C. 2000. Fluoride removal from waters by Donnan
941 dialysis, *Sep. Purif. Technol.* 18, 1-11.
- 942 30. Lounici, H., Adour, L., Belhocine, D., Elmidaoui, A., Barriou, B., Mameru, N., 2001. Novel
943 technique to regenerate activated alumina bed saturated by fluoride ions, *Chem. Eng. J.* 81, 153-160.
- 944 31. Germes, H., Persin, F., Sandeaux, J., Pourcelly, G., Mountadar, M., 2002. Defluoridation of
945 groundwater by a hybrid process combining adsorption and Donnan dialysis, *Desalination* 145, 287-
946 291.
- 947 32. Annouar, S., Mountadar, M., Soufiane, A., Elmidaoui, A., Sahli, M.A.M, Menkouchi, A., 2004.
948 Defluoridation of underground water by adsorption on the chitosan and by electro dialysis,
949 *Desalination* 165, 437-438.
- 950 33. Sahli, M.A.M., Annouar, S., Tahaikt, M., Mountadar, M., Soufiane, A., Elmidaoui, A. 2007. Fluoride
951 removal for underground backish water by adsorption on the natural chitosan and by electro dialysis,
952 *Desalination* 212, 37-45.

- 953 34. Elazhar, F., Tahaikt, M., Zouahri, A., Taky, M., Hafsi, M., Elmidaoui, A. 2013. Defluoridation of
954 Moroccan Groundwater by nanofiltration and electro dialysis: performance and cost comparison,
955 *World Appl. Sci. J.* 22, 844-850.
- 956 35. Mohapatra, M., Anand, S., Mishra, B.K., Giles, D.E., Singh, P., 2009. Review of fluoride removal
957 from drinking water, *J. Environ. Man.* 91, 67-77.
- 958 36. Elazhar, F., Tahaikt, M., Achatei, A., Elmidaoui, F., Taky, M., Hannouni, F.E. Laaziz, I., Jariri, S.,
959 Amrani, M.E., Elmidaoui, A., 2009. Economical evaluation of the fluoride removal by nanofiltration,
960 *Desalination* 24, 154-157.
- 961 37. Nasr, A.B., Charcosset, C., Amar, R.B., Walha, K., 2013. Defluoridation of water by nanofiltration, *J.*
962 *Fluorine Chem.* 150, 92-97.
- 963 38. Ku, Y., Chiou, H.M., Wang, W., 2002. The removal of fluoride ion from aqueous solution by a cation
964 synthetic resin. *Sep. Sci. Technol.* 37, 89-103.
- 965 39. Singh, K., Lataye, D.H., Wasewar, K.L., Yoo, C.K., 2013. Removal of fluoride from aqueous
966 solution: status and techniques, *Desalination and Water Treatment* 51, 3233-3247.
- 967 40. Oyango, M.S., Kojima, Y., Aoyi, O., Bernardo, E.C., Mastuda H., 2004. Adsorption equilibrium
968 modeling and solution chemistry dependence of fluoride removal from water by trivalent-cation-
969 exchanged zeolite F-9, *J. Colloid Inter. Sci.* 279, 341-350.
- 970 41. Pan, B., Xu, J., Wu, B., Li, Z., Liu, X., 2013. Enhanced removal of fluoride by polystyrene anion
971 exchanger supported hydrous zirconium oxide nanoparticles, *Environ. Sci. Technol.* 47, 9347-9354.
- 972 42. Viswanathan, N., Meenakshi, S., 2009. Role of metal ion incorporation in ion exchange resin on the
973 selectivity of fluoride, *J. Hazard. Mater.* 162, 920-930.
- 974 43. Fan, X. Parker, D.J., Smith M.D., 2003. Adsorption kinetics of fluoride on low cost materials. *Water*
975 *Res.* 37, 4929-4937.
- 976 44. Pervov, A.G., Dudkin, E.V., Sidorenko, O.A., Antipov, V.V., Khakhanov, A., Makarov, R.I., 2000.
977 RO and NF membrane systems for drinking water production and their maintenance techniques,
978 *Desalination*, 132, 315-321.
- 979 45. Habuda-Stanić, M., Ravančić, M.E., Flanagan, A. 2014. A review on adsorption of fluoride from
980 aqueous solution, *Materials* 7, 6317-6366.
- 981 46. Li, Y.H., Wang, S., Cao, A., Zhao, D., Zhang, X., Xu, C., Luan, Z., Ruan, D., Liang, J., Wu, D., Wei,
982 B., 2001. Adsorption of fluoride from water by amorphous alumina supported on carbon nanotubes,
983 *Chem. Phys. Lett.* 350, 412-416.
- 984 47. Ghorai, S., Pant, K.K., 2004. Investigations on the column performance of fluoride adsorption by
985 activated alumina in a fixed-bed, *Chem. Eng. J.* 98, 165-173.

- 986 48. Leyva Ramos, R., Ovalle-Turrubiarres, J., Sanchez-Castillo, M.A., 1999. Adsorption of fluoride from
987 aqueous solution on aluminum-impregnated carbon. *Carbon* 37, 609-617.
- 988 49. Srimurali, M., Pragathi, A., Karthikeyan, J., 1998. A study on removal of fluoride from drinking
989 water by adsorption onto low-cost materials, *Environ. Pollut.* 99, 285–289.
- 990 50. Reardon, E.J., Wang, Y., 2001. Activation and regeneration of a soil sorbent for defluoridation of
991 drinking water, *Appl. Geochem.* 16, 531–539.
- 992 51. Mahramanlioglu, M., Kizilcikli, I., Bicer, I.O., 2002. Adsorption of fluoride from aqueous solution by
993 acid treated spent bleaching earth, *J. Fluorine Chem.* 115, 41–7.
- 994 52. Raichur, A.M., Basu, M.J., 2001. Adsorption of fluoride onto mixed rare earth oxides, *Sep. Purif.*
995 *Technol.* 24, 121–127.
- 996 53. McKee, R.H., 1934. Removal of fluoride from drinking water. *Ind. Eng. Chem.* 26, 849–50.
- 997 54. Islam, M., Patel, R. K., 2007. Evaluation of removal efficiency of fluoride from aqueous solution
998 using quick lime. *J. Hazard. Mat.* 143, 303-310.
- 999 55. Nath, S.K., Dutta R.K., 2012. Acid-enhanced limestone defluoridation in column reactor using oxalic
1000 acid, *Process Saf. Environ. Prot.* 90, 65-75.
- 1001 56. Badillo-Almaraz, V. E., Flores, J.A., Arriola, H., López F.A., Ruiz-Ramirez, L., 2007. Elimination of
1002 fluoride ions in water for human consumption using hydroxyapatite as an adsorbent, *J. Radioanal.*
1003 *Nucl. Chem.* 271, 741-744.
- 1004 57. Gao, S., Sun R., Wei, Z., Zhao, H., Li, H., Hu, F., 2009. Size-dependent defluoridation properties of
1005 synthetic hydroxyapatite, *J. Fluorine Chem.* 130, 550-556.
- 1006 58. Poinern, G.E.J., Ghosh, M.K., Ng, Y.J., Issa, T.B., Anand, S., Singh, P., 2011. Defluoridation
1007 behavior of nanostructured hydroxyapatite synthesized through an ultrasonic and microwave
1008 combined technique, *J. Hazard. Mater.* 185, 29-37.
- 1009 59. Wang, Y., Chen, N., Wei W., Cui, J., Wei, Z., 2011. Enhanced adsorption of fluoride from aqueous
1010 solution onto nanosized hydroxyapatite by low-molecular-weight organic acids, *Desalination* 276,
1011 161-168.
- 1012 60. Nagappa, B., Chandrappa, G.T., 2007. Mesoporous nanocrystalline magnesium oxide for
1013 environmental remediation, *Microporous Mesoporous Mater.* 106, 212-218.
- 1014 61. Maliyekkal, S.M., Antony, K.R., Pradeep, T., 2010. High yield combustion synthesis of
1015 nanomagnesia and its applications for fluoride removal, *Sci. Total Environ.* 408, 2273-2282.
- 1016 62. Sasaki, K., Fukumoto, N., Moriyama S., Hirajima T., 2011. Sorption characteristics of fluoride on to
1017 magnesium oxide-rich phases calcined at different temperatures, *J. Hazard. Mater.* 191. 240-248.
- 1018 63. Na, C.K., Park, H.J., 2010. Defluoridation from aqueous solution by lanthanum hydroxide, *J. Hazard.*
1019 *Mater.* 183, 512-520.

- 1020 64. Rao, C.R.N., Karthikeyan, J., 2012. Removal of fluoride from water by adsorption onto lanthanum
1021 oxide, *Water Air Soil Pollut.* 223, 1101-1114.
- 1022 65. Tang, Y., Wang, J., Gao, N., 2010. Characteristics and model studies for fluoride and arsenic
1023 adsorption on goethite, *J. Environmental Sci.* 22, 1689-1694.
- 1024 66. Kumar, E., Bhatnagar A., Ji, M., Jung, W., Lee, S.H., Kim, S.J., Lee G., Song, H., Choi, J.Y., Yang,
1025 J.S., Jeon, B.H., 2009. Defluoridation from aqueous solutions by granular ferric hydroxide (GFH),
1026 *Water Res.* 43, 490-498.
- 1027 67. Tang, Y., Guan, X., Wang, J., Gao, N., McPhail, M.R., Chusuei, C.C., 2009. Fluoride adsorption onto
1028 granular ferric hydroxide: Effects of ionic strength, pH, surface loading, and major co-existing
1029 anions, *J. Hazard. Mater.* 171, 774-779.
- 1030 68. Mohapatra, M., Rout, K., Singh, P., Anand, S., Layek, S., Verma, H.C., Mishra, B.K., 2011. Fluoride
1031 adsorption studies on mixed-phase nano iron oxides prepared by surfactant mediation-precipitation
1032 technique, *J. Hazard. Mater.* 186, 1751-1757.
- 1033 69. Dou, X., Mohan, D., Pittman, C.U., Yang, Jr.S., Yang, S., 2012. Remediating fluoride from water
1034 using hydrous zirconium oxide, *Chem. Eng. J.* 198-199, 236-245.
- 1035 70. Swain, S.K., Patnaik, T., Singh, V.K., Jha, Usha, Patel, R.K., Dey, R.K., 2011. Kinetics, equilibrium
1036 and thermodynamic aspects of removal of fluoride from drinking water using meso-structured
1037 zirconium phosphate, *Chem. Eng. J.* 171, 1218-1226.
- 1038 71. Wajima, T., Umata, Y., Narita, S., Sugawara, K., 2009. Adsorption behavior of fluoride ions using a
1039 titanium hydroxide-derived adsorbent, *Desalination* 249, 323-330.
- 1040 72. Gong, W.X., Qu, J.H., Liu, R.P., Lan, H.C., 2012. Adsorption of fluoride onto different types of
1041 aluminas, *Chem. Eng. J.* 189-190, 126-133.
- 1042 73. Goswami, A., Purkait, M.K., 2012. The defluoridation of water by acidic alumina, *Chem. Eng. Res.*
1043 *Des*, 90, 2316-2324.
- 1044 74. Kamble, S.P., Deshpande, G., Barve, P.P., Rayalu, S., Labhsetwar, N.K., Malyshev, A., Kulkarni,
1045 B.D., 2010. Adsorption of fluoride from aqueous solution by alumina of alkoxide nature: Batch and
1046 continuous operation, *Desalination* 264, 15-23.
- 1047 75. Kumar, E., Bhatnagar, A., Kumar, U., Sillanpää, M., 2011. Defluoridation from aqueous solutions by
1048 nano-alumina: Characterization and sorption studies, *J. Hazard. Mater.* 186, 1042-1049.
- 1049 76. Liu, R., Gong, W., Lan, H., Gao, Y., Liu H., Qu, J., 2011. Defluoridation by freshly prepared
1050 aluminum hydroxides, *Chem. Eng. J.* 175, 144-149.
- 1051 77. Mulugeta, E., Zewge, F., Johnson C.A., Chandravanish, B.S., 2014. A high-capacity aluminum
1052 hydroxide-based adsorbent for water defluoridation, *Desalination and Water Treatment*, 52, 5422-
1053 5429.

- 1054 78. Wang, S.G, Ma, Y., Shi, Y.J., Gong, W.X., 2009. Defluoridation performance and mechanism of
1055 nano-scale aluminum oxide hydroxide in aqueous solution, *J. Chem. Technol. Biotechnol.* 84, 1043-
1056 1050.
- 1057 79. Srivastav, A.L., Singh, P.K., Srivastava V., Sharma Y.C., 2013. Application of a new adsorbent for
1058 fluoride removal from aqueous solutions, *J. Hazard. Mater.* 263, 342-352.
- 1059 80. Liu, H., Deng, S., Li, Z., Yu, G., Huang, J., 2010. Preparation of Al-Ce hybrid adsorbent and its
1060 application for defluoridation of drinking water, *J. Haz. Mat.* 179, 424-430.
- 1061 81. Maliyekkal, S.M., Sharma, A.K., Philip, L., 2006. Manganese-oxide coated alumina: a promising
1062 sorbent for defluoridation of water, *Water Res.* 20, 3497-3506.
- 1063 82. Tripathy, S.S., Raichur, A.M., 2008. Abatement of fluoride from water using manganese dioxide-
1064 coated activated alumina, *J. Haz. Mat.* 153, 1043-1051.
- 1065 83. Bansiwala, A., Pillewan, P., Biniwale, R.B., Rayalu, S.S., 2010. Copper oxide incorporated
1066 mesoporous alumina for defluoridation of drinking water, *Microporous Mesoporous Mater.* 129, 54-
1067 61.
- 1068 84. Deng, S., Liu, H., Zhou, J., Huang, J., Yu, G., 2011. Mn-Ce oxide as a high-capacity adsorbent for
1069 fluoride removal from water, *J. Haz. Mat.* 186, 1360-1366.
- 1070 85. Lin, C., He, B.Y., He, S. Wang, T.J., Su, C., Jin, Y., 2012. Fe-Ti oxide nano-adsorbent synthesized
1071 by co-precipitation for fluoride removal from drinking water and its adsorption mechanism, *Powder*
1072 *Technol.* 227, 3-8.
- 1073 86. Biswas, K., Gupta, K., Ghosh, U.C., 2009. Adsorption of fluoride by hydrous iron(III)-tin(IV)
1074 bimetal mixed oxide from the aqueous solutions, *Chem. Eng. J.* 149, 196-206.
- 1075 87. Biswas, K., Bandhoyadhyay, D., Ghosh, U.C., 2007. Adsorption kinetics of fluoride on iron(III)-
1076 zirconium(IV) hybrid oxide, *Adsorption*, 13, 83-94.
- 1077 88. Dou, X., Zhang, Y., Wang, H., Wang, T., Wang, Y., 2011. Performance of granular zirconium-iron
1078 oxide in the removal of fluoride from drinking water, *Water Res.* 45, 3571-3578.
- 1079 89. Zhijian, L.L., Deng, S., Zhang, X., Zhou, W., Huang, J., Yu, G., 2010. Removal of fluoride from
1080 water using titanium-based adsorbents, *Front. Environ. Sci. Engin. China* 4, 414-420.
- 1081 90. Lin, C., He, S.B.Y., Wang, T.J., Su, C.L., Zhang, C., Yong, J., 2012. Synthesis of iron-doped
1082 titanium oxide nanoadsorbent and its adsorption characteristics for fluoride in drinking water, *Ind.*
1083 *Eng. Chem. Res.* 51, 13150-13156.
- 1084 91. Biswas, K., Saha, S.K., Ghosh, U.C., 2007. Adsorption of fluoride from aqueous solution by a
1085 synthetic Iron(III)-Aluminium(III) mixed oxides, *Ind. Eng. Chem. Res.* 46, 5346-5356.
- 1086 92. Zhao, X., Wang, J., Wu, F., Wang, F., Cai, Y., Shi, Y., Jiang, G., 2010. Removal of fluoride from
1087 aqueous media by Fe₃O₄@Al(OH)₃ magnetic nanoparticles, *J. Haz. Mat.* 173, 102-109.

- 1088 93. Chai, L., Wang, Y., Zhao, N., Yang, W., You, X., 2013. Sulfate-doped $\text{Fe}_3\text{O}_4/\text{Al}_2\text{O}_3$ as a novel
1089 adsorbent for fluoride removal from drinking water, *Water Res.* 47, 4040-4049.
- 1090 94. Kim, J.H., Lee, C.G., Park, J.A., Kang, J.K., Yoon, S.Y., Kim, S.B., 2013. Fluoride removal using
1091 calcinated Mg/Al layered double hydroxides at high fluoride concentration, *Water Sci. Technol.*
1092 *Water Suppl.* 1, 249-256.
- 1093 95. Kang, D., Yu, X., Tong, S., Ge, M., Zuo, J., Cao, C., Song, W., 2013. Performance and mechanism of
1094 Mg/Fe layered double hydroxides for fluoride and arsenate removal from aqueous solution. *Chem.*
1095 *Eng. J.* 228, 731-740.
- 1096 96. Luv, L., He, J., Wei, M., Evans, D.G., Zhou, Z., 2007. Treatment of high fluoride concentration water
1097 by MgAl- CO_3 layered double hydroxides: kinetic and equilibrium studies, *Water Res.* 41, 1534-1542.
- 1098 97. Batistella, L., Venquiaruto, L.D., Di Luccio, M., Oliveira, J.V., Pergher, S.B.C., Mazutti, M.A., de
1099 Oliveira, D., Mossi, A.J., Treichel, H., Dallago, R., 2011. Evaluation of acid activation under the
1100 adsorption capacity of double layered hydroxides of Mg-Al CO_3 type for fluoride removal from
1101 aqueous medium. *Ind. Eng. Chem. Res.* 50, 6871-6876.
- 1102 98. Zhang, T., Li, Q., Xiao, H., Mei, Z., Lu, H., Zhou, Y., 2013. Enhanced fluoride removal from water
1103 by non-thermal plasma modified $\text{CeO}_2/\text{Mg-Fe}$ layered double hydroxides, *Appl. Clay Sci.* 72, 117-
1104 123.
- 1105 99. Zhang, T., Li, Q., Xiao, H., Mei, Z., Lu, H., Zhou, Y., 2012. Synthesis of Li-Al layered hydroxide
1106 (LDHs) for efficient fluoride removal, *Ind. Eng. Chem. Res.* 51, 11490-11498.
- 1107 100. Dey, S., Goswami, S., Gosh, U.C. 2004. Hydrous ferric oxide (HFO)-A scavenger for fluoride from
1108 contaminated water, *Water Air Soil Poll.* 158, 311-323.
- 1109 101. Wu, X., Zhang, Y., Dou, X., Yang, M., 2007. Fluoride removal performance of a novel Fe-Al-Ce
1110 trimetal oxide adsorbent. *Chemosphere* 69, 1758-1764.
- 1111 102. Wu, X., Zhang, Y., Dou, X., Zhao, B., Yang, M., 2013. Fluoride adsorption on an Fe-Al-Ce trimetal
1112 hydrous oxide: Characterization of adsorption sites and adsorbed fluorine complex species. *Chem.*
1113 *Eng. J.* 223, 364-370.
- 1114 103. Biswas, K., Gupta, K., Goswami, A., Ghosh, U.C., 2010. Fluoride removal efficiency from aqueous
1115 solution by synthetic iron(III)-aluminum (III)-chromium(III) ternary mixed oxide. *Desalination* 255,
1116 44-51.
- 1117 104. Sivasankar, V., Muruges, S., Rajkumar, S., Darchen, A., 2013. Cerium dispersed in carbon (CeDC)
1118 and its adsorption behavior: A first example of tailored adsorbent for fluoride removal from drinking
1119 water. *Chem. Engine J.* 214, 45-54.

- 1120 105. Hernández-Montoya, V., Ramírez-Montoya, L.A., Bonilla-Petriciolet, A., Montes-Duran M.A., 2012.
1121 Optimizing the removal of fluoride from water using new carbons obtained by modification of nut
1122 shell with a calcium solution from egg shell, *Biochem. Eng. J.* 62, 1-7.
- 1123 106. Tchomgui-Kamga, E., Alonzo, V., Nansou-Nijiki, C.P., Audebrand, N., Ngameni, E., Darchen, A.
1124 2010. Preparation and characterization of charcoals that contain dispersed aluminium oxide as
1125 adsorbent for removal from drinking water, *Carbon* 48, 333-343.
- 1126 107. Ma, Y., Wang S.G., Fan, M., Gong, W.X., Gao B.Y.. 2009. Characteristics and defluoridation
1127 performance of granular activated carbons coated with manganese oxides, *J. Hazard. Mater.* 168,
1128 1140-1146.
- 1129 108. Janardhana, C., Rao, G.N., Sathish, R.S., Kumar, P.S., Kumar, V.A., Madhav, M.V., 2007. Study on
1130 defluoridation of drinking water using zirconium ion impregnated activated charcoals *Indian J.*
1131 *Chem. Technol.* 14, 350–354.
- 1132 109. Sathish, R.S., Sairam, S., Raja, V.G., Rao, G.N., Janardhana C., 2008. Defluoridation of water using
1133 zirconium impregnated coconut fiber carbon, *Sep. Purif. Technol.* 43, 3676-3694.
- 1134 110. Alagumuthu, G., Rajan, M., 2010. Equilibrium and kinetics of adsorption of fluoride onto zirconium
1135 impregnated cashew nut shell carbon. *Chem. Eng. J.* 158, 451-457.
- 1136 111. Li, Y., Du, Q., Wang, J., Liu, T., Sun, J., Wang, Y., Wang Z., Xia, Y., Xia, L., 2013. Defluoridation
1137 from aqueous solution by manganese oxide coated graphene oxide, *J. Fluorine Chem.* 148, 67-73.
- 1138 112. Velazquez-Jimenez, L.H., Hurt, R.H., Matos, J., Rangel-Mendez, J.R., 2014. Zirconium-carbon
1139 hybrid sorbent for removal of fluoride from water: oxalic acid mediated Zr(IV) assembly and
1140 adsorption, *Eviron. Sci. Technol.* 48, 1166-1174.
- 1141 113. Gupta, R. Ahuja, P., Khan, S., Saxena, R.K., Mohapatra, H., 2000. Microbial biosorbents: meeting
1142 challenges of heavy metal pollution in aqueous solutions, *Curr. Sci.*, 78, 967–973.
- 1143 114. Mehta, S.K., Gaur, J.P., 2001. Characterization and optimization of Ni and Cu sorption from aqueous
1144 solution by *Chlorella vulgaris*, *Ecol. Eng.* 18, 1–13.
- 1145 115. Ilhami, T., Gulay, B., Emine, Y., Gokben, B., 2005. Equilibrium and kinetic studies on biosorption of
1146 Hg (II), Cd (II) and Pb (II) ions onto micro algae *Chlamydomonas reinhardtii*, *J. Environ. Manage.*
1147 77, 85–92.
- 1148 116. Crist, R.H., Oberholser, K., Shank, N., Nguyen, M., 1981. Nature of binding between metallic ions
1149 and algal cell walls, *Environ. Sci. Technol.* 15, 1212–1217.
- 1150 117. Hunt, S., Eccles, H. Diversity of Bio Polymers Structure and its Potential for Ion-Bonding
1151 Applications, *Immobilization of Ions by Biosorption*, Ellies Horword, Chichester (1986), pp. 15–46.
- 1152 118. Mohan, S.V., Karthikeyan, J., 2000. Removal of diazo dye from aqueous phase by algae spirogyra
1153 species, *Toxicol. Environ. Chem.* 74, 147–154.

- 1154 119. Mohan, S.V., Ramanaiah, S.V., Rajkumar, B., Sarma, P.N., 2007. Biosorption of fluoride from
1155 aqueous phase onto Algal *Spirogyra* sp. and evaluation of adsorption kinetics, *Bioresour. Technol.*
1156 98, 1006–1011.
- 1157 120. Mohan, S.V., Ramanaiah, S.V., Rajkumar, B., Sarma, P.N., 2007. Removal of fluoride from aqueous
1158 phase by biosorption onto algal biosorbent *Spirogyra* Sp. I02: sorption mechanism elucidation, *J.*
1159 *Hazard. Mater.* 141, 465–474.
- 1160 121. Mohan, S.V., Bhaskar, Y.V., Karthikeyan, J., 2003. Biological decolorization of simulated azo dye in
1161 aqueous phase by algae *Spirogyra* species, *Int. J. Environ. Pollut.* 21, 211–222.
- 1162 122. Mohan, S.V., Karthikeyan, J., 2000. Removal of diazo dye from aqueous phase by algae *spirogyra*
1163 species, *Toxicol. Environ. Chem.*, 74, 147–154.
- 1164 123. Jamode, B., Chandak, S., Rao, M., 2004. Evaluation of performance and kinetic parameters for
1165 defluoridating using *Azadirachta Indica* (Neem) leaves as low cost adsorbents, *Pollut. Res.*, 23, 239–
1166 250.
- 1167 124. Yao, R., Meng, F., Zhang, L., Ma, D., Wang, M., 2009. Defluoridation of water using neodymium-
1168 modified chitosan, *J. Hazard. Mater.* 165, 454–460.
- 1169 125. Sundaram, C.S., Viswanathan, N., Meenakshi, S., 2008. Uptake of fluoride by nano-
1170 hydroxyapatite/chitosan, a bioinorganic composite, *Bioresour. Technol.* 99, 8226–8230.
- 1171 126. Sundaram, C.S., Viswanathan, N., Meenakshi, S., 2009. Defluoridation of water using
1172 magnesia/chitosan composite, *J. Hazard. Mater.* 163, 618–624.
- 1173 127. Sundaram, C.S., Viswanathan, N., Meenakshi, S., 2009. Fluoride sorption by nano-
1174 hydroxyapatite/chitin composite, *J. Hazard. Mater.* 172, 147–151.
- 1175 128. Jagtap, S., Thakre, D., Wanjari, S., Kamble, S., Labhsetwar, N., Rayalu, S., 2009. New modified
1176 chitosan-based adsorbent for defluoridation of water, *J. Colloid Interface Sci.* 332, 280–290.
- 1177 129. Kamble, S.P., Jagtap, S., Labhsetwar, N.K., Thakare, D., Godfrey, S., Devotta, S., Rayalu, S.S., 2007.
1178 Defluoridation of drinking water using chitin, chitosan and lanthanum-modified chitosan, *Chem. Eng.*
1179 *J.* 129, 173–180.
- 1180 130. Bansiwala, A., Thakre, D., Labhsetwar, N., Meshram, S., Rayalu, S., 2009. Fluoride removal using
1181 lanthanum incorporated chitosan beads, *Colloids Surf., B: Biointerfaces* 74, 216–224.
- 1182 131. Thakre, D., Jagtap, S., Bansiwala, A., Labhsetwar, N., Rayalu, S., 2010. Synthesis of La-incorporated
1183 chitosan beads for fluoride removal from water, *J. Fluorine Chem.* 131, 373–377.
- 1184 132. Jagtap, S., Yenkie M.K., Das, S., Rayalu, S., 2011. Synthesis and characterization of lanthanum
1185 impregnated chitosan flakes for fluoride removal in water, *Desalination* 273, 267–275.
- 1186 133. Viswanathan, N., Meenakshi, S., 2008. Enhanced fluoride sorption using La(III) incorporated
1187 carboxylated chitosan beads, *J. Colloid Interface Sci.* 322, 375–383.

- 1188 134. Viswanathan, N., Meenakshi, S., 2009. Synthesis of Zr(IV) entrapped chitosan polymeric matrix for
1189 selective fluoride sorption, *Colloids Surf. B: Biointerfaces* 72, 88-93.
- 1190 135. Liu, B., Wang D., Yu, G., Meng, X., 2013. Removal of F⁻ from aqueous solution using Zr(IV)
1191 impregnated dithiocarbamate modified chitosan beads, *Chem. Eng. J.* 228, 224-231.
- 1192 136. Swain, S. K., Dey R.K., Islam M., Patel, R.K., Jha, U, Patnaik, T., Airoidi, C., 2009. Removal of
1193 Fluoride from Aqueous Solution Using Aluminum-Impregnated Chitosan Biopolymer, *Sep. Sci.*
1194 *Technol.* 44, 2096-2116.
- 1195 137. Viswanathan, N., Meenakshi, S., 2010. Enriched fluoride sorption using alumina/chitosan composite,
1196 *J. Hazard. Mater.* 178, 226-232.
- 1197 138. Ramanaiah, S.V., Mohan, S.V., Sarma, P.N., 2007. Adsorptive removal of fluoride from aqueous
1198 phase using waste fungus (*Pleurotus ostreatus* 1804) biosorbent: Kinetics evaluation, *Ecol Eng.* 31,
1199 47-56.
- 1200 139. Yu, X., Tong, S., Ge, M., Zuo, J., 2013. Removal of fluoride from drinking water by
1201 cellulose@hydroxyapatite nanocomposites, *Carbohydr. Polym.* 92, 269-275.
- 1202 140. Zhao, Y., Li, X., Liu, L., Chen, F., 2008. Fluoride removal by Fe(III)-loaded ligand exchange cotton
1203 cellulose adsorbent from drinking water, *Carbohydr. Polym.* 72, 144-150.
- 1204 141. Suzuki, T., Nakamura, A., Niinae M., Nakata, H., Fujii, H., Tasaka, Y., 2013. Immobilization of
1205 fluoride in artificially contaminated kaolinite by the addition of commercial-grade magnesium oxide,
1206 *Chem. Eng. J.* 233, 176-184.
- 1207 142. Xu, X., Li, Q., Cui, H., Pang, J., Sun, L., An, H., Zhai, J., 2011. Adsorption of fluoride from aqueous
1208 solution on magnesia-loaded fly ash cenospheres, *Desalination* 272, 233-239.
- 1209 143. Paudyal, H., Pangeni, B., Inoue, K., Kawakita, H., Ohto, K., Alam, S., 2013. Adsorptive removal of
1210 fluoride from aqueous medium using a fixed bed column packed with Zr(IV) loaded dried orange
1211 juice residue, *Biores. Technol.* 146, 713-720.
- 1212 144. Paudyal, H., Pangeni, B., Ghimire, K.N., Inoue, K., Ohto, K., Kawakita, H., Alam, S., 2012.
1213 Adsorption behavior of orange waste gel for some rare earth ions and its application to the removal of
1214 fluoride from water, *Chem. Eng. J.* 195-196, 289-296.
- 1215 145. Ganvir, V., Das, K., 2011. Removal of fluoride from drinking water using aluminum hydroxide
1216 coated rice husk ash, *J. Haz. Mater.* 185, 1287-1294.
- 1217 146. Wang, X.H., Song, R.H., Yang, H.C., Shi, Y.J., Dang, G.B., Yang, S., Zhao, Y., Sun, X.F., Wang,
1218 S.G., 2013. Fluoride adsorption on carboxylated aerobic granules containing Ce(III), *Biores. Technol.*
1219 127, 106-111.
- 1220 147. Sujana, M.G., Mishra, A., Acharya, B.C., 2013. Hydrous ferric oxide doped alginate beads for
1221 fluoride removal: adsorption kinetics and equilibrium studies, *Appl. Surf. Sci.* 270, 767-776.

- 1222 148. Huo, Y., Ding, W., Huang, X., Xu, J., Zhao, M., 2011. Fluoride Removal by Lanthanum Alginate
1223 Bead: Adsorbent Characterization and Adsorption Mechanism, *Chin. J. Chem. Eng.* 19, 365-370.
- 1224 149. Zhou, Y., Yu, C., Shan, Y., 2004. Adsorption of fluoride from aqueous solution on La³⁺-impregnated
1225 cross-linked gelatin, *Sep. Purif. Technol.* 36, 89-94.
- 1226 150. Chen, N., Zhang, Z., Feng, C., Li, M., Zhu, D., Sugiura, N., 2011. Studies on fluoride adsorption of
1227 iron impregnated granular ceramics from aqueous solution, *Mater. Chem. Phys.* 125, 293-298.
- 1228 151. Swain, S.K., Mishra, S., Patnaik, T., Patel, R.K., Jha, U., Dey, R.K., 2012. Fluoride removal
1229 performance of a new hybrid sorbent of Zr(IV)-ethylenediamine, *Chem. Eng. J.* 184, 72-81.
- 1230 152. Samatya, S., Mizuki, H., Io, Y., Kawakita, H., Uezu, K., 2010. The effect of polystyrene as a porogen
1231 on the fluoride ion adsorption of Zr(IV) surface-immobilized resin, *React. Funct. Polym.* 70, 63-68.
- 1232 153. Xu, Y.M., Ning, AR., Zhao, J., 2001. Preparation and Defluorination Performance of Activated
1233 Cerium(IV) Oxide/SiMCM-41 Adsorbent in Water, *J. Colloid Interface Sci.* 235, 66-69.
- 1234 154. Islam, M., Mishra, P. C., Patel, R., 2011. Fluoride adsorption from aqueous solution by a hybrid
1235 thorium phosphate composite, *Chem. Eng. J.* 166, 978-985.
- 1236 155. Fang, L., Ghimire K.N., Kuriyama, M., Ioue, K., Makino, K., 2003. Removal of fluoride using some
1237 lanthanum(III)-loaded adsorbents with different functional groups and polymer matrices, *J. Chem.*
1238 *Technol. Biotechnol.* 78, 1038-1047.
- 1239 156. Chen, N., Feng, C., Li, M., 2014. Fluoride removal on Fe-Al-impregnated granular ceramic adsorbent
1240 from aqueous solution, *Clean Technol. Environ. Policy.* 16, 609-617.
- 1241 157. Wu, H.-X., Wang, T.-J., Chen, L., Jin, Y., Zhang, Y., & Dou, X.-M., 2011. Granulation of Fe-Al-Ce
1242 hydroxide nano-adsorbent by immobilization in porous polyvinyl alcohol for fluoride removal in
1243 drinking water. *Powder Technology*, 209(1-3), 92-97.

Table 1. Summary of the most common water treatment technologies for fluoride removal [8, 13, 45].

Technology	Advantages	Disadvantages
Coagulation/Precipitation	Widely used, high efficiency, commercially available technique	Could be expensive due to the large amounts of chemical required, efficiency depends of pH and presence of co-ions in water to be treat, adjustment and readjustment of pH is required. Formation of toxic sludge that requires it disposal. Low effectiveness (cannot remove F below 5 mg L ⁻¹).
Membrane processes: reverse osmosis, nanofiltration	High efficiency, remove other contaminants. No chemicals required.	High capital investment due to the operational (energy) and maintenance cost. Toxic waste water is produced due to F concentrated residue. No ion selectively. Some membranes are pH sensitive. Clogging, scaling and fouling problems.
Electrochemical treatments: dialysis, electro dialysis	High efficiency and selectivity. No chemical required. No waste production	High cost during installation, operation (energy) and maintenance. No ion selectivity. Skilled labor required. Polarization problems.
Ion exchange	High efficiency, simplicity and flexibility of design,	Expensive due to the resins, vulnerable to interfering ions (sulfate, phosphate, chloride, bicarbonate, etc.). Replacement of media after multiple regenerations, produces toxic liquid waste, and the efficiency is highly pH-dependent.
Adsorption	Greater accessibility and low cost due to the wide range of adsorbents, simple operation.	High efficiency often demands adjustment and readjustment of pH, some water ions can interfere in fluoride adsorption. Replacement of media after multiple regenerations. Disposal of used adsorbent.

Table 2. Adsorption capacities and other parameters for the removal of fluoride by selected monometallic adsorbents.

Adsorbent	Fluoride adsorption capacity/ mg g ⁻¹	Optimal pH	Temperature/°C	Reference
Lanthanum hydroxide	242.2	7.5	25	[63]
Granular ferric hydroxide	7.0	4-8	25	[66]
Zirconium oxide	68	7	25	[69]
Alumina hydroxide	110	5.0-7.2	25	[76]
Nano-AlOOH	3.26	7	---	[78]

Table 3. Adsorption capacities and other parameters for the removal of fluoride by selected multimetallic impregnated adsorbents.

Adsorbent	Fluoride adsorption capacity/ mg g ⁻¹	Optimal pH	Temperature/°C	Reference
Al-based material modified with Ce	62	6	25	[80]
Al-Mn hybrid material	2.852	4-7	30	[81]
MnO ₂	0.16	7	25	[82]
Powder Mn-Ce material mixed with pseudo-bohemite (AlOOH)	79.5	6	25	[84]
Hydrous Fe(III)-Zr(IV) hybrid oxide	7.51	6.8	20	[87]
Iron doped Ti(IV)	53.22	7	25	[90]
Fe(III)-Al(III)	17.73	6.9	28	[91]
Fe ₂ O ₃ /Al(OH) ₃ nanoparticles	88.49	6.5	25	[92]
Sulfate doped Fe ₂ O ₃ /Al(OH) ₃	70.4	7	25	[93]
MgAl-CO ₃	319.8	6	30	[96]
CeO ₂ /Mg-Fe layered double hydroxide composite	52.4	6-7	25	[98]
Li-Al double hydroxide composite	42.43	7	40	[99]
Synthetic hydrated iron(III)-aluminum(III)-chromium(III) ternary mixed oxide	31.88	4-7	30	[103]

Table 4. Adsorption capacities and other parameters for the removal of fluoride by carbon based adsorbents.

Adsorbent	Fluoride adsorption capacity/ mg g ⁻¹	Optimal pH	Temperature/°C	Reference
Cerium dispersed in carbon	52	8	25	[104]
CMPNS-4	2.3	7	30	[105]
Al-Fe impregnated activated carbon	13.64	7	28 ± 2	[106]
Granular activated carbons coated with manganese oxides	2.24	5.2	28	[107]
Zirconium impregnated coconut fiber carbon	20.109	8	rt*	[109]
Zirconium impregnated cashew nut shell carbon	1.83	7	30	[110]
Manganese oxide coated graphene oxide	11.93	5.5-6.7	---	[111]
Zirconium-carbon hybrid sorbent	5.94	7	25	[110]

*room temperature

Table 5. Adsorption capacities and other parameters for the removal of fluoride by biosorbents and natural materials modified with metals.

Adsorbent	Fluoride adsorption capacity/ mg g ⁻¹	Optimal pH	Temperature/°C	Reference
neodymium-modified chitosan	22.38	7	50	[124]
Nano-hydroxyapatite/chitosan	1.56	7	30	[125]
Magnesia/chitosan composite	11.236	10.1-10.4	30	[126]
Magnesia/chitin composite	2.840	7	30	[127]
Modified chitosan-based adsorbent	9.0	7.03	30±2	[128]
Lanthanum-modified chitosan	3.1	6.7	30±2	[129]
Lanthanum incorporated chitosan beads	4.7	5	30±1	[130]
La-incorporated chitosan beads	4.7	---	30±1	[131]
Lanthanum impregnated chitosan flakes	1.27	---	---	[132]
La(III)-incorporated carboxylated chitosan beads	4.711	Neutral pH	30	[133]
Zr(IV) entrapped chitosan polymeric matrix	4.850	Neutral pH	30	[134]
Zr(IV) impregnated dithiocarbonate modified chitosan beads	4.58	7	30	[135]
Aluminum-Impregnated Chitosan Biopolymer	1.73	6.7	25±2	[136]
Alumina/chitosan composite	3.81	Neutral pH	30	[137]

Table 5. Adsorption capacities and other parameters for the removal of fluoride by biosorbents and natural materials modified with metals. (Continuation)

Adsorbent	Fluoride adsorption capacity/ mg g^{-1}	Optimal pH	Temperature/ $^{\circ}\text{C}$	Reference
Fungal <i>Pleurotus ostreatus</i> 1804 SP as biosorbents	1.27	7	30	[138]
cellulose@hydroxyapatite nanocomposites	4.22	6.5	25±1	[139]
Fe(III)-loaded ligand exchange cotton cellulose adsorbent	18.6	5.6	25	[140]
Magnesia-loaded fly ash cenospheres	6.0	3	45	[142]
Zr(IV) loaded dried orange juice residue	13.9	4	rt*	[143]
Sc-Saponified orange juice residue	0.6 (mmol/g)	4	30	[144]
Jm- Saponified orange juice residue	1.22 (mmol/g)	5	30	[144]
La- Saponified orange juice residue	1.06 (mmol/g)	4	30	[144]
Ho- Saponified orange juice residue	0.92(mmol/g)	4	30	[144]
Aluminum hydroxide coated rice husk ash	15	5	27±1	[145]
Carboxylated aerobic granules containing Ce(III)	45.80	Neutral pH	25±1	[146]
Hydrous ferric oxide doped alginate beads b	8.9	7	29	[147]
Lanthanum Alginated Beads	197.2	4	25	[148]
La ³⁺ -impregnated cross-linked gelatin	21.28	5-7	29	[149]

*room temperature

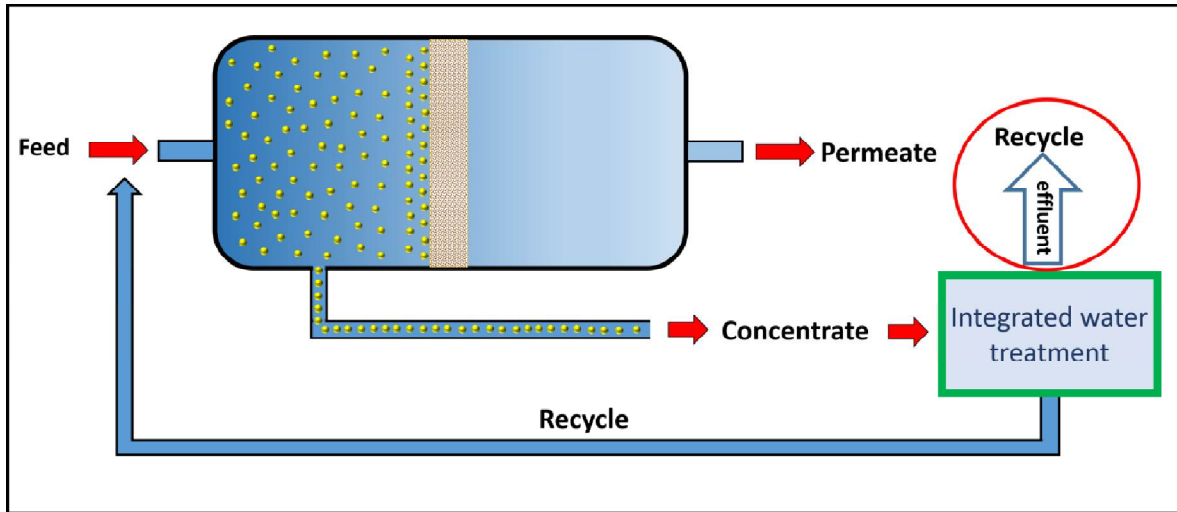
Table 6. Adsorption capacities and other parameters for the removal of fluoride by modified synthetic resins, ceramics and polymers.

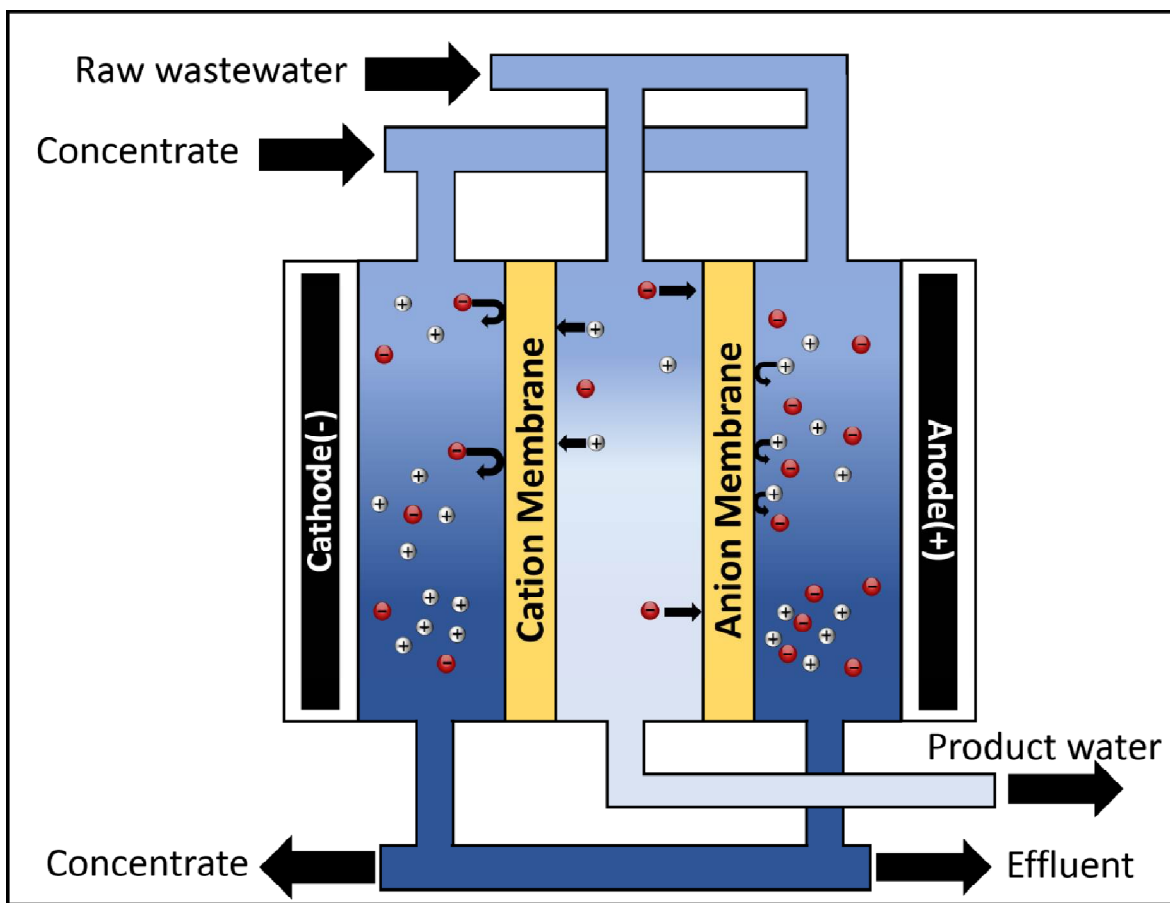
Adsorbent	Fluoride adsorption capacity/ mg g ⁻¹	Optimal pH	Temperature/°C	Reference
FeSO ₄ ·7H ₂ O impregnated granular ceramics	2.157	6.9±0.1	30	[20]
Fe ₂ O ₃ impregnated granular ceramics	1.699	6.9±0.1	30	[150]
Zr(IV)-ethylenediamine	37.03	7	25±2	[151]
Zr(IV) surface immobilized	5.52	---	30	[152]
Activated Cerium(IV) oxide/SiMCM-41	5-6 (mmol/g)	---	20	[153]
Thorium phosphate composite	4.74	Neutral pH	25±2	[154]
200CT resin loaded with lanthanum	1.34	6	30	[155]
Fe-Al-impregnated granular ceramic adsorbent	3.56	6.9±0.1	25±1	[156]
Fe-Al-CE hydroxide nanoadsorbent-polyvinyl alcohol	4.46	6.5	25	[157]

Figure 1. Schematic representation of reverse osmosis.

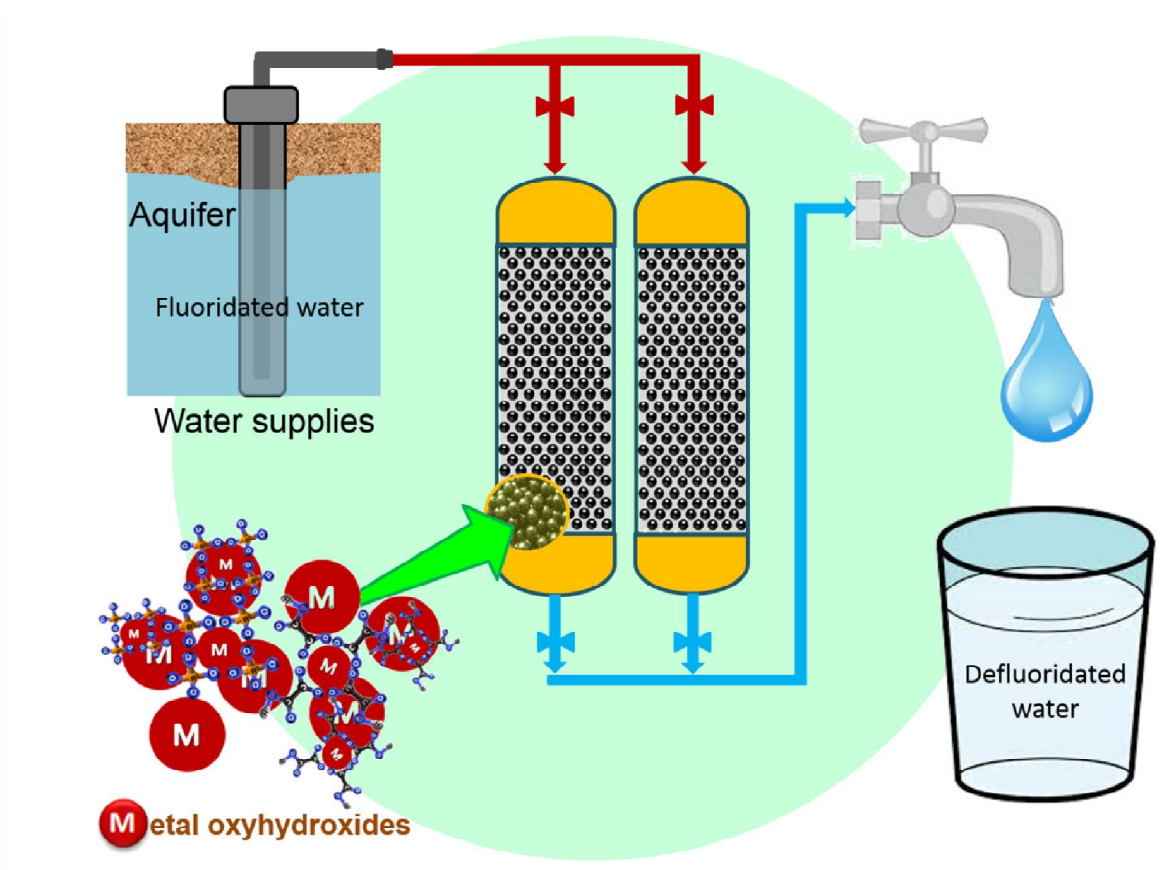
Figure 2. Schematic representation of electrodialysis.

ACCEPTED MANUSCRIPT





ACCEPTED



ACCEPTED

Highlights

- Efforts to reduce fluoride from drinking water to acceptable limits are essential.
- More efficient and cost-effective materials are needed for water defluoridation.
- Adsorption is an important process to remove fluoride from water.
- Metal oxyhydroxides have a high potential for water defluoridation.



ACCEPTED MANUSCRIPT